Research Article

SufB intein splicing in *Mycobacterium tuberculosis* is influenced by two remote conserved N-extein Histidines

Running Title: Conserved histidines regulate *Mtu* SufB cleavage

Sunita Panda[1†], Ananya Nanda[1†], Nilanjan Sahu[2],Deepak Ojha[1], Biswaranjan Pradhan[3], Anjali Rai[1], Amol R. Suryawanshi[4], Nilesh Banavali[5,6] and Sasmita Nayak[1*]

[1]School of Biotechnology, Kalinga Institute of Industrial Technology, Bhubaneswar, Odisha, India 751024,

[2]School of Biological Sciences, National Institute of Science Education and Research Bhubaneswar, Jatni, Khurda, Odisha, India 752050

[3] S K Dash center of excellence of Biosciences and Engineering & Technology, School of Basic Sciences, Indian Institute of Technology Bhubaneswar, Argul, Khurda, Odisha, India 752050

[4] Clinical Proteomics, Institute of Life Sciences, Bhubaneswar, Odisha 751023 India

[5] Laboratory of Cellular and Molecular Basis of Diseases, Division of Transitional Medicine, Wadsworth Center, New York State Department of Health, Empire State Plaza, Albany New York 12237

[6] Department of Biomedical Sciences, School of Public Health, 1 University Place, Rensselaer, New York 12144

[†] These authors contributed equally: Sunita Panda, Ananya Nanda.

[*]Correspondence: Dr. Sasmita Nayak, School of Biotechnology, Kalinga Institute of Industrial Technology, Campus XI, Patia, Bhubaneswar, Odisha, India 751024

Email:-sasmita.n@kiitbiotech.ac.in; Tel: +918763000005

Abbreviations:

Mtu: *Mycobacterium tuberculosis*

WT: Wild type

SI: Splicing inactive

DM: *Mtu* SufB Double mutant

IPTG: Isopropyl β- d-1-thiogalactopyranoside

TCEP: Tris (2-carboxyethyl) phosphine

HA: Hydroxylamine

DTT: Dithiothreitol

HRP: Horseradish peroxidase

ECL: Enhanced chemiluminescence

TBST: Tris-buffered saline, 0.1% tween 20

BSA: Bovine serum albumin

ß-gal: Beta galactosidase

ABC: Ammonium bicarbonate

ACN: Acetonitrile

TFA: Tri-fluoro acetic acid

HPLC: High pressure (or performance) liquid chromatography

FPLC: First protein liquid chromatography

MALDI-TOF/TOF: Matrix assisted laser desorption ionization time-of-flight

SDS: Sodium dodecyl sulphate

PAGE: Polyacrylamide gel electrophoresis

RMSD: Root mean square deviation

SASA: Solvent accessible surface area

RMSF: Root mean square fluctuation

PME: Particle-mesh Ewald

HPCC: High performance computing cluster

MD Simulations: Molecular dynamic simulations

Abstract: Inteins are auto-processing domains that implement a multi-step biochemical reaction termed protein splicing, marked by cleavage and formation of peptide bonds. They excise from a precursor protein, generating a functional protein via covalent bonding of flanking exteins. We report the kinetic study of splicing and cleavage reaction in [Fe-S] cluster assembly protein SufB from *Mycobacterium tuberculosis*. Although it follows a canonical intein splicing pathway, distinct features are added by extein residues present in the active site. Sequence analysis identified two conserved histidines in the N-extein region; His-5 and His-38. Kinetic analyses of His-5Ala and His-38Ala SufB mutants exhibited significant reductions in splicing and cleavage rates relative to the SufB wild-type precursor protein. Structural analysis and molecular dynamics simulations suggested that *Mtu* SufB displays a unique mechanism where two remote histidines work concurrently to facilitate N- terminal cleavage reaction. His-38 is stabilized by the solvent-exposed His-5, and can impact N-S acyl shift by direct interaction with the catalytic Cys1. Development of inteins as biotechnological tools or as pathogen specific novel antimicrobial targets requires a more complete understanding of such unexpected roles of conserved extein residues in protein splicing.

Keywords: Intein splicing; Splicing regulation; conserved histidines; *Mycobacterium tuberculosis* SufB; SufB intein.

1. Introduction

Protein splicing is a self-catalyzed event that generates a continuous extein protein by ligating two intein separated extein regions with a peptide bond. This post-translational auto-excision of the intervening intein protein is critical for the formation of an active protein(1-4). Splicing and cleavage products (Figure 1C) are obtained through a series of nucleophilic displacement

reactions mediated in a coordinated fashion by the catalytic residues(5-9). Control over this reversible interruption of the functional form of the host exteins can play a regulatory role in protein activation (10, 11). The extein sequences upstream and downstream of N-terminal and C-terminal intein ends are termed 'N-extein' and 'C-extein' respectively. The intein folds into a horseshoe-shaped structure with a catalytic cleft that brings the conserved catalytic residues and the extein splice junction close enough for initiation of splicing reaction(12).

Inteins themselves have N-terminal and C-terminal regions with conserved sequence segments (termed as Blocks or motifs) that facilitates the splicing and cleavage reaction(s). N-terminal intein region comprises of A, N2, B, and N4 structural motifs or Blocks while F- and G-Blocks are part of the C-terminal intein region (13). Typically, A-Block contains Cys/Ser or Thr; B-Block includes His and Thr residues; F-Block usually has Asp and His and the G-Block bears two conserved residues; a penultimate His and a terminal Asn (8, 14, 15). Classical or Canonical (Class 1) intein splicing involves 4 sequential acyl rearrangements (Figure 1C), a nucleophilic attack by C1 or S1/T1 leads to an N-S/N-O acyl shift converting the peptide bond of N-terminal splice junction to a thioester linkage, a second nucleophilic attack by C+1 forms a branched intermediate at C-terminal splice junction through esterification, the branched intermediate is resolved by terminal Asn cyclization through cleavage of C-terminal splice junction, and finally an (S-N/O-N) acyl shift fully ligates the two extein segments by an amide bond formation (16-18).

These bond rearrangements at splice junctions during the cleavage and splicing reaction(s) are assisted by non-catalytic intein residues through stabilization of various intermediate structure(s)(19).The Block A residues Cys, Ser, or Thr participate in the first step of splicing with significant assistance from the Block B His and Thr residues. The highly conserved Block

B His destabilizes the scissile peptide bond either by reducing the energy barrier or by loss of resonance or protonation of the Cys1 amide bond via His imidazole ring to catalyze the N-S acyl shift (20-24).The Block F Asp residue drives the thio-esterification through the tetrahedral intermediate by ground-state destabilization (8, 22, 25). It is also proposed that Block B histidine plays a dual catalytic role; being weakly basic it deprotonates the Cys1 to accelerate the N-S acyl shift and subsequently acts as an acid to stabilize the tetrahedral intermediate(21, 23, 24). The Block F Asp residue also deprotonates the C+1 residue to stabilizes the net positive charge on Cys1 that drives the transesterification reaction. The F- and G-Block His residues are critical in the coordination of terminal Asn cyclization. The F-Block His increases nucleophilicity of Asn, and the G-Block His accelerates the Asn cyclization by increasing the electrophilicity of backbone peptide (26-29). The final acyl-shift is energetically favorable and does not require assistance from either intein or extein residues(30). Inteins do show polymorphisms in the catalytic residues leading to variation in the splicing mechanism as seen in Class 2 and Class 3 intein splicing (11, 31-35).

Interactions between extein residues and the catalytic intein core in the regulation of splicing reaction have been studied by modulating intein activity, changing the conformation of catalytic cleft, and restraining the activity of catalytic residues (6, 15, 36-39). Previous studies on intein-extein partnership in intein splicing have suggested mediation by extein residues both near and remote to the N- and C-terminal splice junctions (7, 15, 36, 38, 40-42).The N-extein residue at the first position (-1) is important for the first thioester reaction and shows enhanced N-terminal cleavage rate (>4-fold) or attenuated cleavage by 1,000-fold by replacing the native residue to aspartate and proline respectively (36). Substitution of bulky amino acids at this position can cause local distortion and induce N-cleavage reaction (23). The participation of the first C-

extein Cys+1 in the second and third steps of the splicing reaction has been demonstrated by its mutation dramatically augmenting or inhibiting splicing and generating off-pathway N-cleavage products(12, 14, 17, 40, 43). Earlier, extein effects were assumed to be limited to residues proximal to the intein (12, 15, 44), but recent work has shown that distal exteins are implicated as environmental sensors with the role in regulating splicing depending on solution environment and temperature in *Pho* RadA precursors (6, 10, 39).

SufB is a critical component of [Fe-S] cluster assembly and repair machinery called SUF (mobilization of sulfur) complex. This is a stress response system that gets upregulated during periods of oxidative stress and Fe starvation (45, 46). Though there are multiple pathways for [Fe-S] cluster biogenesis among the three kingdoms of life such as NIF (nitrogen fixation) and ISC (Iron-sulfur cluster), the SUF complex is unique in mycobacteria. Fe-S cluster containing proteins execute a broad spectrum of cellular functions in organisms such as respiration, gene regulation, RNA modification, DNA repair, and replication (47-49). Although the SUF system has been well characterized in the *E. coli* system,(17, 45, 46, 50-52), the importance of SufB intein splicing in the formation of functional Suf complex has been shown in mycobacteria (52).

The present study reports on the splicing and cleavage reactions of a full-length *Mtu* SufB (FL-SufB) precursor protein. We delineated the different structural domains of *Mtu* SufB, analyzed whether it follows a canonical or non-canonical intein splicing pathway, identified intein and extein residues that participate in catalytic cleft formation, assessed both their conservation in different mycobacterial species and their role in regulating cleavage and/or splicing reactions, and analyzed distinctions from other intein precursor proteins. We found intein residues highly conserved in different mycobacterial species that favor a canonical splicing mechanism (Figure 1A and 1B). We detected two distal histidines in the N-extein region, His-5 and His-38, that are

conserved in mycobacteria, archaea, and other microbes where SUF is the exclusive system for Fe-S cluster biogenesis (Figure 2A and 2B). Biochemical analyses of H-5A and H-38A SufB mutants confirmed their influence on splicing and cleavage. Structural modeling of *Mtu* SufB and explicit-solvent molecular dynamics (MD) simulations of the model were used to analyze the SufB precursor splicing active site dynamics, and these simulations suggested that N-terminal cleavage could be supported by an interaction between H-38 and H-5. These observations suggest that the two distal H-5 and H-38 N-extein residues participate in SufB precursor stabilization and aid *Mtu* SufB intein splicing.

Kinetic analyses of H-5A SufB mutant demonstrated 3-fold and 1.4-fold reductions in splicing and cleavage rates respectively, relative to wild-type *Mtu* SufB precursor. Likewise, a 3.4-fold and 3-fold reduction in splicing and cleavage rates were observed in the H-38A SufB mutant. A side-by-side *Mtu* SufB structure prediction was done using homology (chimera) modeling, secondary structure prediction through consensus with other protein sequences. Subsequently, molecular dynamics (MD) simulations in aqueous media were carried out to find the equilibrated structure. Furthermore, MD simulations clarified the structural features of the SufB intein active site and indicated that N-terminal cleavage reaction is catalyzed by H-38 with the assistance of H-5. Taken together, our study substantiates a distinct mechanism for N-terminal cleavage reaction shown by *Mtu* SufB. Although H-38 is relatively distal to the N-terminal splice junction when supported by His-5, it can efficiently activate the first step of splicing reaction. Finally, we have proposed a novel mechanism for the N-cleavage reaction mediated via the concerted actions of these conserved histidines in the N-extein region of *Mtu* FL-SufB precursor. These observations suggest that H-5 and H-38 might have important biological role(s) in the SufB precursor stabilization and perhaps the functionality of *Mtu* SufB protein.

2. MATERIALS AND METHODS

2.1. Genetic constructs

The full-length Fe-S cluster assembly protein SufB from the *Mycobacterium tuberculosis* H37Rv strain (*Mtu* FL-SufB) and its isolated intein (*Mtu*-SufB-I) genes were PCR-amplified using Pfu Ultra High-Fidelity DNA Polymerase (Agilent Technologies) from heat-killed *Mtu* genomic DNA. DNA purification by gel electrophoresis was followed by EcoRI and HindIII restriction digestion and cohesive end ligation (T4 DNA Ligase, NEB Cat. No. M0202S) for cloning. The genes were inserted into the multiple cloning site 1 (MCS1) of the low copy expression vector pACYCDuetTM-1(Novagen), which was driven by a T7 promoter/lac operator with a chloramphenicol resistance gene for selection. The constructs were screened via colony PCR and confirmed by sequencing (Sequencing Core Facility, SUNY, Albany, and Eaton Bioscience Inc. sequencing service) using the ACYCDuetUP1 (Novagen Cat. No.71178-3) and DuetDOWN1 primers (Novagen Cat. No. 71179-3), as well as the original primers. *Mtu* FL-SufB mutants H5A, H38A, C1A, N359A were generated by substituting respective key catalytic residues to alanine via phosphorylated inverse PCR primers. Splicing inactive (SI) *Mtu* FL-SufB double mutant (C1A/N359A) was created via inverse PCR to add the N359A mutation into the C1A cleavage mutant. The cloned H-38A SufB mutant genes were also confirmed separately by sequencing (Agrogenomics, Odisha) using ACYCDuetUP1 (IDT Cat. No. 103948189) and DuetDOWN1 (IDT Cat. No. 103948190) along with the SufB Primers. All the above primers are listed in Table S1 (Supplementary materials).

2.2. Sequence analysis

Protein sequences for *Mtu* FL- SufB (Accession number YP_006514844.1, GI: 397673309) and the 477 amino acid intein-less SufB protein from *Mycobacterium smegmatis* strain MC2 155 (*Msm*-SufB-FL, accession number YP_887437.1, GI: 118472504) were pairwise sequence aligned in ClustalW to distinguish extein and intein regions in *Mtu* FL-SufB (53). The identified *Mtu* SufB intein sequence (*Mtu* SufB-I) was confirmed by sequence comparison using Blast with the sequences deposited in Inbase (The Intein Database, www.inteins.com) (54). Different structural domains of the intein-like homing endonuclease, and the N- and C-terminal inteins were clearly demarcated by sequence alignment and structural analysis of SufB intein with homing endonuclease domain (I-CreI) and intein homing endonuclease Ii (PDB: 2CW7). The *Mtu* SufB-FL and *Msm*-SufB-FL sequences, combined with one archaeal and other bacterial SufB proteins collected from the NCBI and intein databases (54), were aligned using Dialign2 software (55). Conservation of different intein and extein residues was edited and color-coded manually. Phylogenetic tree analysis was performed using the Maximum likelihood method in the MEGA X program (56, 57) for both SufB inteins [Figure 2C (ii)] and SufB precursor sequences [Figure 2C (i)] from different organisms.

2.3. Protein overexpression and purification

Full-length (FL) un-spliced precursor and mutant SufB proteins carrying an N-terminal 6X-His-tag were over-expressed in BL21 (DE3) *E.coli* cells via IPTG (500µM) (Sigma 367-93-1) induction at 37°C for 4hrs. Cells were resuspended in lysis buffer (20mM sodium phosphate, 0.5M NaCl, pH 7.4) and lysed via tip sonicator (Sonics vibra cell VCX-130). Proteins were over-expressed and isolated from inclusion bodies (IB) via centrifugation. The IB materials were

solubilized by 8M urea (23) (Merck, 1084870500) buffer (lysis buffer, 8M urea, 20 mM of imidazole (MP–biochemicals-288-32-4) and centrifuged at 16,500g for 20 min to collect the supernatant. Then 6X-His-tagged wild type SufB precursor and mutant proteins were purified by Ni-NTA affinity column (Ni-NTA His trap, HP GE Healthcare Life Sciences-17524802) (23, 58-62). Prior to sample application, columns were equilibrated with binding buffer (20mM sodium phosphate, 0.5M NaCl, 40mM imidazole). After sample loading, columns were washed several times (15 CV) in binding buffer. Finally, proteins were eluted as purified fractions in elution buffer (20mM sodium phosphate, 0.5M NaCl, 500mM imidazole) followed by quantification via Bradford's assay.

2.4. *In-vitro* splicing and cleavage assays

2.5 µM of purified proteins were allowed to refold in 1ml of renaturation buffer (20 mM sodium phosphate, 0.5 M NaCl, 0.5 M Arginine,1 mM EDTA, pH 7.4) in presence of 2mM TCEP-HCl (sigma-51805-45-9) at 20˚C for 24h (58-63). The 0hr sample was retrieved before renaturation and splicing was quenched by addition of loading dye (0.1% bromophenol blue, 50% glycerol, ß-mercaptoethanol, 10% SDS, tris 6.8) followed by rapid freezing at -20°C. Our controls, splicing inactive(SI) SufB double mutant and empty expression vector pACYC Duet-1, were treated similarly for the *in-vitro* assays. For the N-cleavage assay, proteins were refolded in presence of reducing agents and nucleophiles such as 2mM TCEP-HCl, 50 mM DTT (Roche-10708984001), and 0.5 M 250 Hydroxylamine (SRL-66164) with 1mM TCEP in renaturation buffer (58-63). For splicing and cleavage analysis, sample extraction at each time interval was followed by the addition of loading dye to stop the reactions and then boiling at 95˚C for 5 min. Resultant products from various refolding reactions were resolved through 4~10% gradient SDS PAGE. Protein bands were stained with Coomassie blue R-250 and densitometric analysis was

performed by using GelQuant.Net biochemical solutions. Percentage(s) of splicing and cleavage products were measured by taking the percentage(s) of the ratio of the total splicing product (LE and I) over total proteins (LE+I+P) and total N-cleavage product (NE+NC) over total proteins (NE+NC+P). The 0hr splicing value(s) were subtracted at each time point for baseline correction.

2.5. Kinetic analyses

Since *Mtu* 6X (His)-tagged WT SufB and SufB mutants (H-5A, H-38A, and SI C1A/N359A) were purified and renatured at different temperatures, after normalizing splicing and cleavage values at different time intervals, the plot was generated by taking the percentage of splicing or cleavage product with respect to time (in min). Next, the curve was fitted in pseudo-first-order kinetics, with an equation Y=Y0 + (Plateau-Y0) *(1-exp(-K*x)) [Where X=time, Y0 =Y value when time (X)= time0, Plateau= max Y value at time t, K = rate constant, expressed in reciprocal of the X-axis (time units)] in graph pad prism software. The fitted curve was generated by automatic outlier elimination fitting in a nonlinear regression equation. The rate constant (K) and Vmax were generated by the software. Half-life (t1/2) was calculated by graph pad prism using the formula (Ln2/K).

2.6. Western blot

Western blot analysis was performed using an anti-His antibody (Invitrogen, LOT 1902132) to confirm the identity of splicing and cleavage products. Following resolution through SDS PAGE, test proteins were transferred to a nitrocellulose membrane; at 50v, 2h. After a successful transfer, blocking was done with 5% skim milk for 2h at room temperature. Then the blot was incubated with HRP conjugated anti-His antibody (Invitrogen, LOT 1902132) at 1:5000 dilutions

for 16h at 40 C. Then blot was washed with 1X TBST and developed using 13 ECL as the substrate. N-extein detection was done with 1:2500 antibody dilution.

2.7 Mass spectrometry and chromatography

After renaturation, proteins were resolved through 4~10% SDS PAGE. Protein identification by mass spectrometry was performed at Central Proteomics Facility, Institute of Life Sciences, Bhubaneswar. In gel digestion of protein and extraction followed the protocol described by Shevchenko et. al. (64). Extracted peptides were desalted by using C18 Zip-Tip (Millipore) and then dried in a centrifugal vacuum concentrator. Peptide samples were reconstituted with 0.1% TFA in 50% ACN solution, mixed (1:1) with α-cyano-4-hydroxycinnamic acid solution (C8982; 10 mg/ml) and then spotted onto metal target plate in triplicates. MS and MS/MS spectra were acquired using MALDI TOF/TOF (AbSciex TOF/TOF 5800). Acquired spectra were searched against *Mycobacterium tuberculosis* from NCBInr database using Mascot search algorithm (version 2.0; Matrix Science, Boston, Massachusetts) and protein pilot software (SCIEX, USA) for protein identification (65, 66). Searches were performed allowing trypsin mis-cleavage up to 1; Carbamido-methylation of cysteine and oxidation of methionine as variable and fixed modification respectively. The peptide mass tolerance was set as 100 ppm for precursor ion and 0.8 Da for fragment ion with +1 charge. Since all the splicing and cleavage products were identified as *Mtu* FL-SufB, the acquired spectra were researched against a customized database containing probable splicing products and cleavage products of SufB protein of *Mycobacterium tuberculosis* using mascot search engine in Protein Pilot Software with the same parameter. β-gal and BSA were run as internal calibration. The protein score, percent coverage, theoretical molecular weight, and Iso-electric pH value were obtained. The mass spectrometry proteomics

data have been deposited to the ProteomeXchange Consortium via the PRIDE [1] partner repository with the dataset identifier PXD015199.

Purified and renatured *Mtu* FL-SufB protein was examined by analytical HPLC carried out on an Agilent 1200 series instrument equipped with a Zorbax gf-450 column (6µm, 9.4x250mm) with a flow rate of 1ml/min. All HPLC runs used the following solvent: 1:1 water and isopropanol (solvent 1) and 0.1% TFA (Trifluoroacetic acid)in water (solvent 2). The column was equilibrated using solvent 1 and solvent 2. A protein sample was inserted into the column and ran for 30mins. The retention time vs protein intensity measured at 280 nm was noted. For reference, we ran 6µl of Precision plus protein ladder (Biorad1610374) diluted to 30µl using Sodium phosphate buffer. The retention time vs molecular weight of the known protein standards was measured and plotted to make a standard curve. The unknown protein peaks from the test samples were compared with the standard curve to find out the relative molecular weights. The molecular weights of the expected fragments from the MALDI-TOF/TOF MS (Table S3) data were compared with the standard curve and molecular weights of the unknown peaks were determined.

2.8 Molecular Dynamics (MD) Simulations

2.8.1. Homology modeling of Mtu SufB precursor

A homology model of the *Mtu* FL-SufB precursor was built using the SufB chain of the *E. coli* SufB-SufC-SufD complex (PDB ID: 5AWF, chain A), the *S. cerevisiae* intein homing endonuclease (PDB ID: 1VDE, chain A), and the *T. kodakarensis* homing endonuclease (PDB ID: 2CW7, chain A) using Bioluminate 2.7 from Schro□dinger. The model was assessed by Ramachandran plot analysis and PROSA(Z-score) (67).

2.8.2. MD simulation analysis

Explicit-solvent MD simulations were performed using GROMACS (V5.1.4) (68) with the OPLS-AA force field (69) and the SPC/E water model (70, 71). The *Mtu* SufB model (846 aa) was solvated in a cubic box with at least 1 nm distance between the protein and the edge of the box, and neutralized with NaCl. The system was minimized with target Fmax of no greater than 1000 kJ mol-1 349 nm-1 with steepest descent minimization with a spherical cut-off at 1 nm was imposed on all intermolecular interactions with verlet cut-off scheme(72, 73). The leap-frog algorithm with a timestep of 2fs (74) and a canonical NVT ensemble was used to run the simulation for 100 ns, with temperature maintained at 300K through velocity-rescale coupling and no temperature coupling. H-bonds were constrained using lincs with the order of 4 (75). The particle-mesh Ewald (PME) algorithm was used for implementing long-range electrostatic interactions with the grid dimension of 0.16nm and interpolation order of 4 (76). Histidine at positions 5 and 36 were mutated to alanine by homology modelling, and MD simulations were performed on these mutant proteins in an identical fashion. The MD simulation trajectories were analyzed with GROMACS (68) and PyMOL Molecular Graphics System, Version 1.2r3pre, Schrödinger, LLC, and plotted using Origin 8.0.

3. RESULTS

3.1 Structural domains of *Mtu* full-length (FL) SufB precursor

Pair-wise sequence alignment of the *Mtu*-FL-SufB and the intein-less *Msm*-FL-SufB protein sequences using Clustal-W could delineate the intein and extein boundaries for *Mtu*-FL-SufB due to the ~95% sequence similarity between the extein sequences. The boundaries of the 359 amino acid *Mtu* SufB (*Mtu* Pps1) intein from *M. tuberculosis* strain H37Rv were also affirmed

by a Blast search of Inbase. The final demarcation of these structural domains is shown in Table S2 and is illustrated in Figure 1A. Multiple sequence alignment with other inteins shows conservation of catalytic cysteines (C1 and C+1), Block B His67, Block F Asp77, penultimate His358, and terminal Asn359 (Figure 1B). The presence of these conserved residues suggests that the *Mtu*-FL-SufB precursor (846 aa) is auto-processed by a canonical intein splicing pathway to ligate its N-extein (252 aa) and C-extein (235 aa) to form the native SufB protein (487 aa). The major by-product is the SufB intein (359 aa) containing an intein domain (155 aa) and an endonuclease domain (204 aa), with minor off-pathway products possible due to N-terminal cleavage (594 aa) and C-terminal cleavage (611 aa) (54, 77).

A

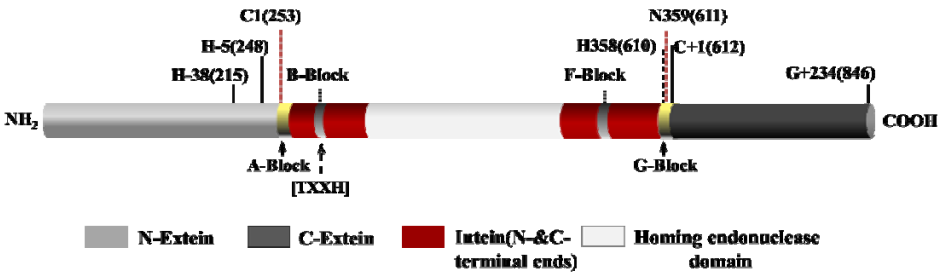

B

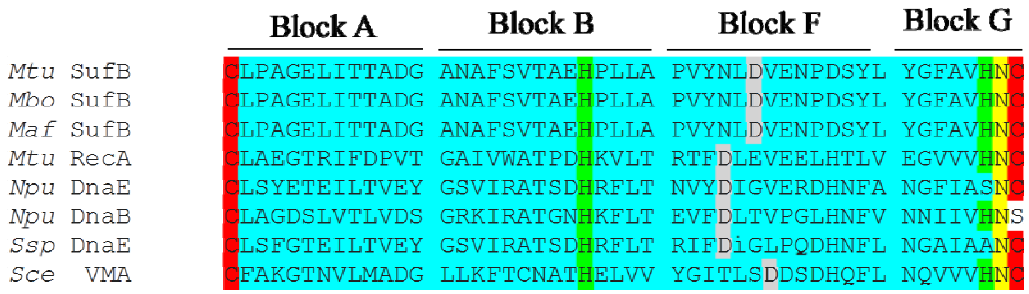

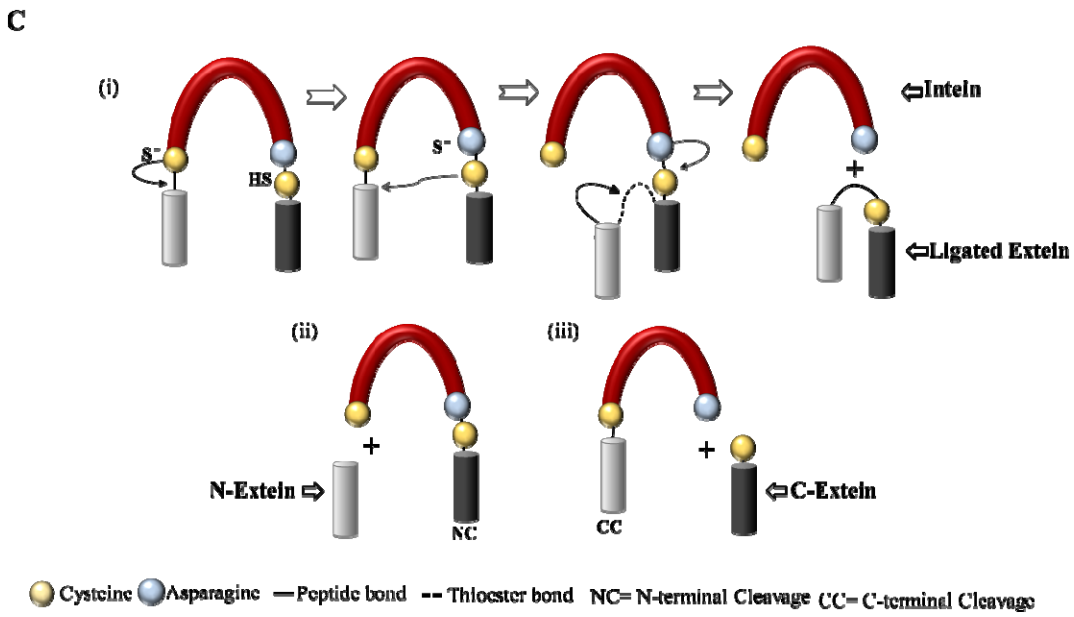

Figure1. (A) Structural domains of the *Mtu* FL-SufB precursor. Important residues for the intein (numbered 1, 2, …), N-extein (numbered -1, -2, …) and C-extein (numbered +1, +2, …) are shown at the top. The conserved N-extein histidines are H-5 (H248 in *Mtu* FL-SufB) and H-38 (H215 in *Mtu* Fl-SufB). (B) Multiple sequence alignment of *Mtu* SufB with other intein-containing precursors shows conserved residues (highlighted in different colors) that participate in a canonical splicing pathway. (C) (i)Mechanism of intein splicing comprising of sequential nucleophilic attacks by C1 and C+1 to generate a branched intermediate by trans-esterification, cyclization of terminal Asn to resolve the branched intermediate ligates exteins and to cleave the SufB intein. (ii) N-terminal and (iii) C-terminal cleavage to form off-pathway products.

3.2 Conservation of His-5 and His-38 in different bacterial species

SufB from different mycobacterial and archaeal species exhibit high sequence similarity (Figure 2A and B). Phylogenetic analysis suggests that these mycobacterial proteins have a common ancestral origin (78). Cladogram analysis of SufB intein sequences from different mycobacterial species shows significant similarities, except in *M. leprae*, *M. lepromatosis*, *M. triplex* and *M. xenopi*, possibly due to different intein insertion sites (17). In Ferroplasma, which belongs to a different kingdom, there is divergence for both the intein [Figure 2C (ii)]

and the full precursor [Figure 2C (i)]. These variations in the extein sequences and intein insertion sites suggests some divergent intein evolution and independent intein transfer in different species and kingdoms.

A

```
M.tuberculosis (206)   ---------- ---------- ----SFIYVP PGVHVDIPLQ AYFRINTENM (231)
M.microti      (206)   ---------- ---------- ----SFIYVP PGVHVDIPLQ AYFRINTENM (231)
M.africanum    (206)   ---------- ---------- ----SFIYVP PGVHVDIPLQ AYFRINTENM (231)
M.bovis        (206)   ---------- ---------- ----SFIYVP PGVHVDIPLQ AYFRINTENM (231)
M.Bourgelatii  (199)   ---------- ---------- ----SFIYVP PGVHVDIPLQ AYFRINTENM (224)
M.Kansasii     (199)   ---------- ---------- ----SFIYVP PGVHVDIPLQ AYFRINTENM (224)
M.orygis       (206)                              SFIYVP PGVHVDIPLQ AYFRINTENM (231)
M.gastri_W     (199)   ---------- ---------- ----SFIYVP PGVHVDIPLQ AYFRINTENM (224)
M.gastri_p     (453)   ---------- ---------- ----SFIYVP PGVHVDIPLQ AYFRINXENM (224)
M.canettii     (211)   ---------- ---------- ----SFIYVP PGVHVDIPLQ AYFRINTENM (236)
M.caprae       (206)   ---------- ---------- ----SFIYVP PGVHVDIPLQ AYFRINTENM (231)
M.Pinnipeddii  (206)   ---------- ---------- ----SFIYVP PGVHVDIPLQ AYFRINTENM (231)
M.xenopi       (578)   ---------- ---------- ----SFIYVP PGVHVEIPLQ AYFRINTENM (603)
M.triplex      (577)   ---------- ---------- ----SFIYVP PGVHVDIPLQ AYFRINTENM (602)
M.leprae       (564)   EKPTYDIQVV GLENFVANGI VAHNSFIYVP PGVHVDIPLQ AYFRINTENM (613)
M.lepromatosis (563)   EKPTYDIQVV GLENFVANGI VAHNSFIYVP PGVHVDIPLQ AYFRINTENM (612)
Ferroplasma    (196)   ---------- ---------- ----SFLYVP KNVTIDMPLQ TYFRMNGEQS (221)

M.tuberculosis (232)   GQFERTLIIA DEGSYVHYVE GCLPAGELIT TADGDLRPIE SIRVGDFVTG (281)
M.microti      (232)   GQFERTLIIA DEGSYVHYVE GCLPAGELIT TADGDLRPIE SIRVGDFVTG (281)
M.africanum    (232)   GQFERTLIIA DEGSYVHYVE GCLPAGELIT TADGDLRPIE SIRVGDFVTG (281)
M.bovis        (232)   GQFERTLIIA DEGSYVHYVE GCLPAGELIT TADGDLRPIE SIRVGDFVTG (281)
M.Bourgelatii  (225)   GQFERTLIIA DEGSYVHYVE GCLPAGELIT TADGDLRPIE SIQVGDYVTG (274)
M.Kansasii     (225)   GQFERTLIIA DEGSYVHYVE GCVPAGELIT TADGDLRPIE SIRVGDYVSS (274)
M.orygis       (232)   GQFERTLIIA DEGSYVHYVE GCLPAGELIT TADGDLRPIE SIRVGDFVTG (281)
M.gastri_W     (225)   GQFERTLIIA DEGSYVHYVE GCLPAGELIT TADGDLRPIE SIRVGDYVTG (274)
M.gastri_p     (479)   GQFERTLIIV GENAYVTYVE G--------- ---------- ---------- (499)
M.canettii     (237)   GQFERTLIIA DEGSYVHYVE GCLPAGELIT TADGDLRPIE SIRVGDFVTG (286)
M.caprae       (232)   GQFERTLIIA DEGSYVHYVE GCLPAGELIT TADGDLRPIE SIRVGDFVTG (281)
M.Pinnipeddi   (232)   GQFERTLIIA DEGSYVHYVE GCLPAGELIT TADGDLRPIE SIRVGDFVTG (281)
M.xenopi       (604)   GQFERTLIIV DENAYVHYVE G--------- ---------- ---------- (624)
M.triplex      (603)   GQFERTLIIV DEGAYVHYVE G--------- ---------- ---------- (623)
M.leprae       (614)   GQFERTLIIA DTGSYVHYVE G--------- ---------- ---------- (634)
M.lepromatosis (613)   GQFERTLIIA DEGSYVHYVE C--------- ---------- ---------- (633)
Ferroplasma    (222)   GQFEHTIVVA DEGAKVHYIE CGLPEDELIS QGDkfv-PIN ELLTDDSVVS (270)
```

B

```
M.tuberculosis (181) EYFGTVIPAGDNKFSALNTAVWSGGSFIYVPPGVHVDIPLQAYFRINTENMGQFERTLII(240)
M.marinum      (174) QYFGTVIPAGDNKFSALNTAVWSGCSFIYVPPGVHVDIPLQAYFRINTENMGQFERTLII(245)
M.fortuitum    (181) KYFGTVIPAGDNKFSALNTAVWSGGSFIYVPPGVHVDIPLQAYFRINTENMGQFERTLII(251)
M.smegmatis    (171) QYFGTVIPAGDNKFSALNTAVWSGCSFIYVPPGVHVDIPLQAYFRINTENMGQFERTLII(241)
M.shigaense    (175) QYFGSVIPAGDNKFSALNTAVWSGGSFIYVPPGVHVDIPLQAYFRINTENMGQFERTLII(245)
S.aureus       (159) KYFASVVPAADNKFAALNSAVWSGGSFIYVPKNIKLDTPLQAYFRINSENMGQFERTLII(229)
B.subtilis     (159) EHWAKVIPPTDNKFAALNSAVWSGGSFIYVPKGVKVETPLQAYFRINSENMGQFERTLII(229)

M.tuberculosis (241) ADEGSYVHYVEGCLPAGELITTADGDLRPIESIRVGDFVTGHDGRPHRVTAVQVRDLDGE(290)
M.marinum      (235) ADEGSYVHYVEG----------------------------------------------(246)
M.fortuitum    (241) ADEGSYVHYVEG----------------------------------------------(252)
M.smegmatis    (231) VDEGAYVHYVEG----------------------------------------------(242)
M.shigaense    (235) VDEGAYVHYVEG----------------------------------------------(246)
S.aureus       (219) ADEGASVHYVEG----------------------------------------------(230)
B.subtilis     (219) VDEEASVHYVEG----------------------------------------------(230)
```

C

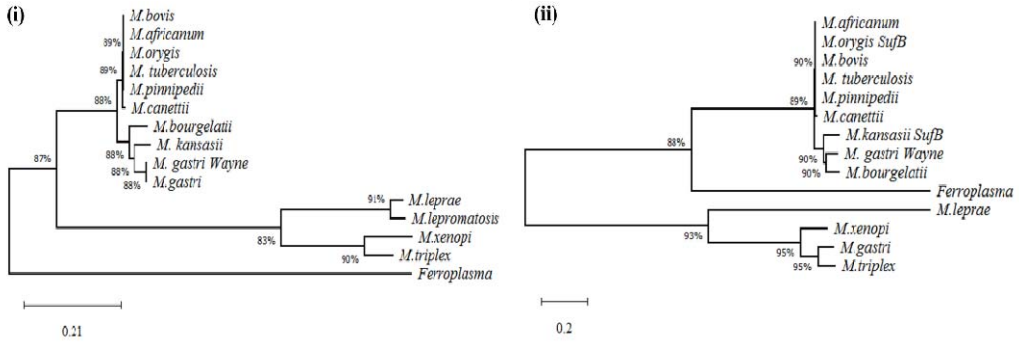

Figure 2. Conserved histidines in the *Mtu* FL-SufB N-extein. (A) Multiple sequence alignment focused on the junction between the N-extein and intein in mycobacterial and archaeal species SufB proteins with conserved H-5 (yellow), H-38 (green), C1 in intein (red). N-extein and intein residues are delineated by shading in grey and cyan blue, (B) Multiple sequence alignment focusing on N-extein~intein junction in mycobacteria and organisms where SUF is the exclusive system for Fe-S cluster assembly, (C) phylogenetic analyses of (i) full-length (FL) SufB protein and (ii) SufB intein sequences in mycobacteria and *Ferroplasma acidarmans*.

Two conserved histidines were identified in the N-extein region of different mycobacterial and archaeal SufB precursor proteins: His-5 and His-38 (Figure 2A). His-5 is conserved in intein-less SufB proteins from *Staphylococcus aureus*, *Bacillus subtilis*, and certain mycobacteria that use SUF complex as the sole pathway for [Fe-S] cluster generation (Figure 2B) (79, 80). His-38 is conserved in both intein-bearing and intein-less mycobacterial SufB proteins where the SUF system is required to synthesize [Fe-S] clusters (Figure 2B). Identification of two highly conserved metal-chelating residues proximal to N-terminal extein~intein junction raises the possibility of their regulatory roles on cleavage and/or splicing as well as in the functionality of

[Fe-S] cluster assembly protein SufB. These two histidines could participate in protein splicing either via direct or indirect interaction with the catalytic residues near cleavage site(s).

3.3 Kinetic study to evaluate the roles of conserved His-5 and His-38 on *Mtu* SufB intein splicing

H-5A and H-38A single mutants were generated to test for a regulatory effect of His-5 and His-38 on *Mtu* SufB intein cleavage and/or splicing. Such alanine substitutions for active site residues have previously resulted in a complete blockage of cleavage and splicing reactions (36). The splicing inactive (SI) SufB double mutant, with both C1 and N359 mutated to alanine (C1A/N359A), which is expected to abolish intein splicing completely (81), was used as a negative control.

Remnant 6x(His)-tagged *Mtu* FL-SufB precursor (P, 95.98 KDa), N-terminal cleavage (NC, 65.26 KDa) product, N-extein (NE, 29.9 KDa), ligated exteins (LE, 55.7 KDa), and intein (I, 40.2 KDa) were all observed upon *in vitro* refolding followed by SDS PAGE, and western blot analysis of the splicing of the *Mtu* FL-SufB precursor and its H-5A and H-38A mutants (Figure 3). As expected, none of the post-reaction products were seen in the case of SI double mutant (Figure S2A) and transformants expressing empty vector pACYC Duet-1 (Figure S2B). Possibly due to protein degradation, the C-terminal cleavage product (CC, 70.12 KDa) and C-extein (CE, 25.76 KDa) were not detected, which precluded analysis of the effects of H-5A and H-38A mutations on C-terminal cleavage.

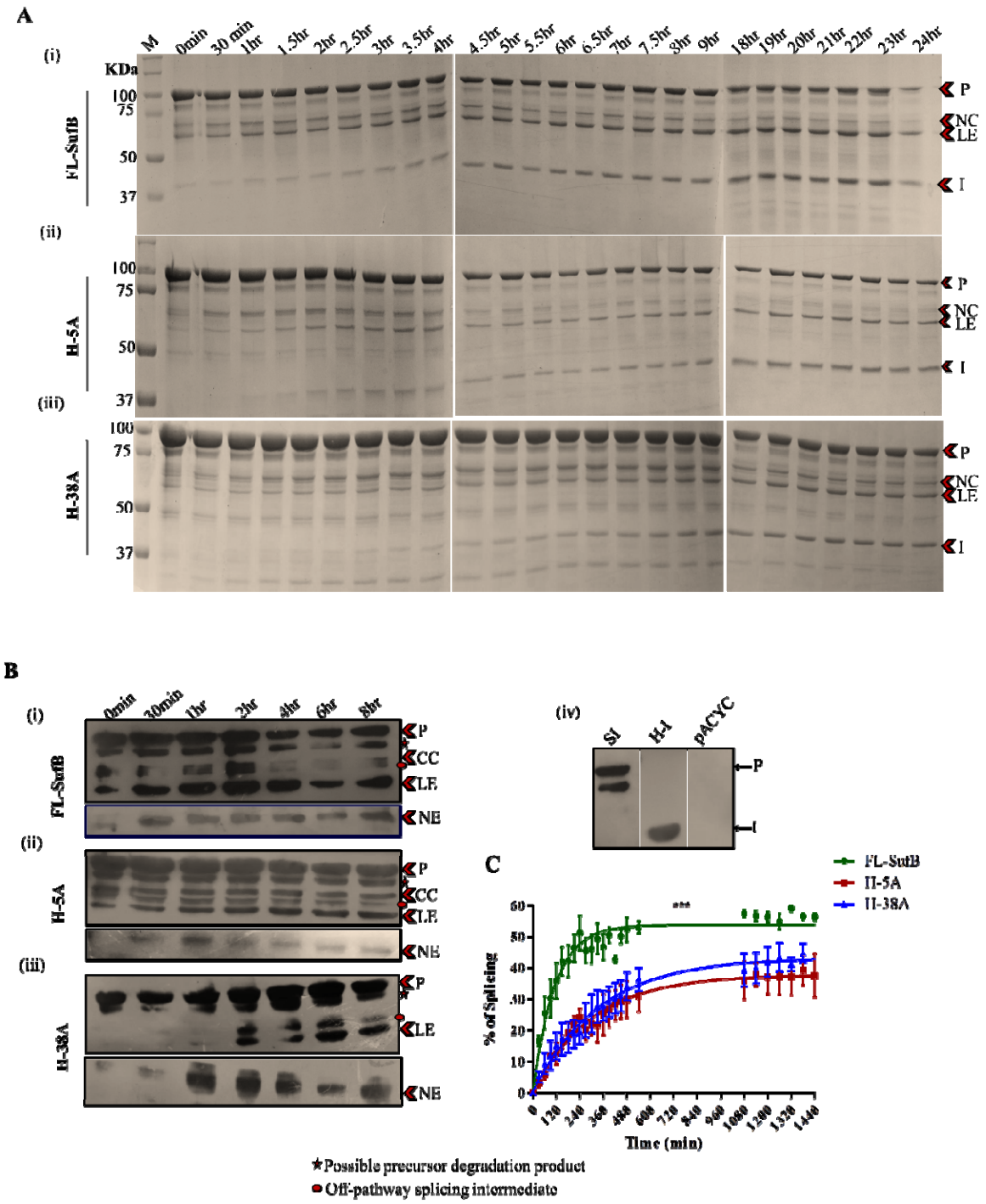

Figure 3. Effect of H-5A and H-38A mutations on *Mtu* SufB splicing. (A) Products from *in vitro* refolding reactions were resolved through 4~10% gradient SDS PAGE for (i) *Mtu* FL-SufB precursor, (ii) H-5A, and (iii) H-38A mutant proteins exhibiting splicing over different time

periods. (B) Western blot using anti-His antibodies confirm the identity of splicing and cleavage products for 6x(His)-tagged (i) *Mtu* FL-SufB precursor,(ii) H-5A,(iii) H-38A and (iv) the controls SI (splicing inactive double mutant SufB), H-I[6x(His)- tagged SufB intein], and pACYC Duet-1(cell lysates expressing empty expression vector). NE was blotted separately with higher concentration of primary antibody. (C) Splicing kinetics in *Mtu* FL-SufB precursor, H-5A, and H-38A with product quantities over different time periods fit to a pseudo first order reaction; Y=Y0 + (Plateau-Y0) *(1-exp(-K*x)).A statistically significant difference in splicing efficiency ($p<0.0001$) is observed between *Mtu* FL-SufB precursor, H-5A and H-38A mutants. Error bars represents (±1) SEM from 3 independent sets of experiments. P=Precursor, CC=C-cleavage, NC=N-cleavage, LE=Ligated Extein, I=Intein, NE=N-Extein, M= Protein marker.

3.3.1 *H-5A and H-38A mutants exhibit attenuated splicing reaction*

Densitometric analysis was performed after *in vitro* renaturation of FL and mutant SufB proteins over a period for 24h. Precursor (P) proteins detected at time 0h were comparable for FL and mutant proteins (Figure 3A). Splicing efficiency was calculated as a percentage of splicing [(I+LE/P+I+LE) x 100] and plotted over time as pseudo-first-order reaction kinetics (Figure 3C). At 20°C, at least 3-fold reductions in splicing efficiency were observed for H-5A and H-38A, relative to *Mtu*-FL-SufB precursor ($p<0.0001$; one-way ANOVA, Table 1).

Table 1. Comparative analysis of different kinetic parameters for splicing in FL-SufB precursor, H-5A and H-38A SufB mutant proteins, at 20 °C temperature (data also shown in Figure 3C).

Kinetic parameters	FL-SufB	H-5A	H-38A
Y_{max}	53.81±1.03	37.82±1.68	43.35±1.7
Rate constant (K) (min^{-1})	$9.92 \pm 0.007 \times 10^{-3}$	$3.3 \pm 0.0003 \times 10^{-3}$	$2.9 \pm 0.0003 \times 10^{-3}$
Half-life($t_{1/2}$)	1.1h	3.4h	3.8h

3.4 Kinetic studies of *Mtu* SufB N-terminal cleavage

The equilibrium of the first N/S acyl transfer step was examined using the reagents DTT (Dithiothreitol), and HA (Hydroxylamine), which induce N-terminal cleavage reaction. DTT can act both as a nucleophile and reducing agent. HA acts as a nucleophile and like DTT targets the linear thioester intermediate in the first step of splicing (82). The reducing agent Tris (2-carboxyethyl) phosphine (TCEP) was used as a control (83). N-cleavage reaction products were analyzed by SDS PAGE (Figure 4, 5, and Figure S3) and densitometric analysis of the cleavage products.

3.4.1 H-5A and H-38A mutations reduce TCEP mediated N-cleavage

The H-5A and H-38A mutant proteins showed diminished production of N-cleavage (NC) products relative to *Mtu* FL-SufB [Figure 4, Table 2(i)], although a proper fit for the reaction time course was not obtained through linear or non-linear regression. In *Mtu*-FL-SufB, N-cleavage was accelerated until 40 min followed by a decline as splicing became distinct. H-5A and H-38A mutants presented a sluggish course with the N-cleavage product peak at 60-80 min and then tapered off. At 40 min and 60 min, H-5A displayed 2-fold and 1.5-fold decrease in % N-cleavage respectively, relative to FL-SufB. Likewise, at 40 min and 60 min, H-38A mutant displayed a 3.8-fold and 3-fold reduction in % of N-cleavage respectively relative to FL-SufB (Figure 4).

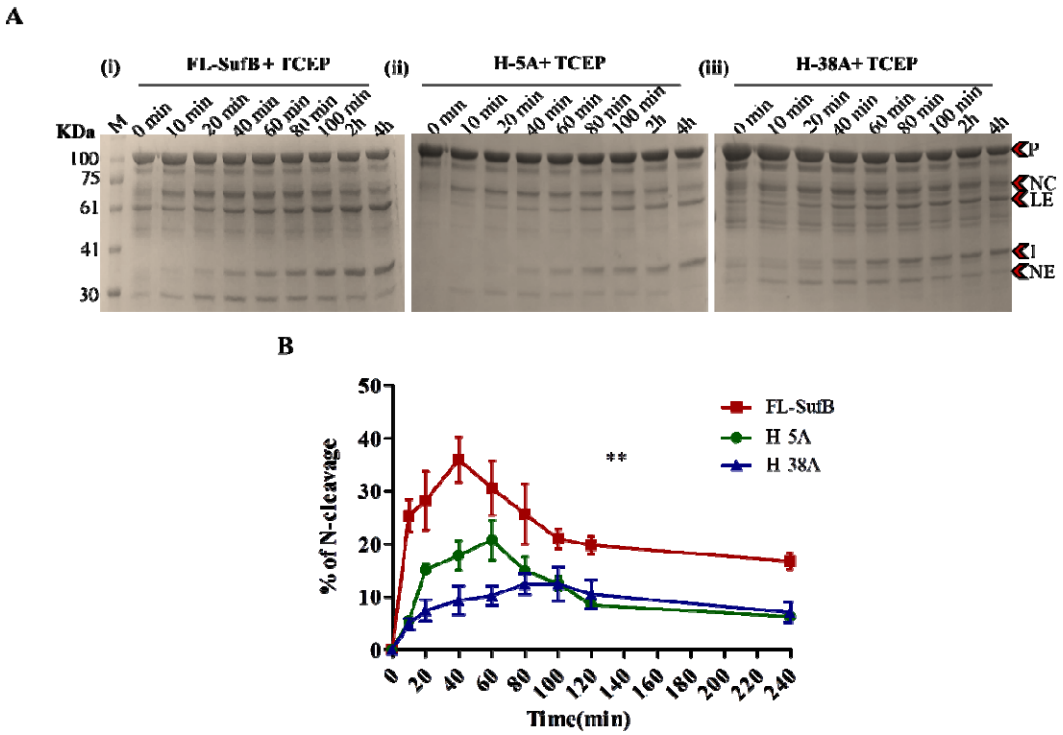

Figure 4. TCEP mediated N-cleavage in *Mtu* SufB:(A) SDS PAGE analysis of (i) *Mtu* FL-SufB precursor, (ii) H-5A and (iii) H-38A proteins displaying N-cleavage reactions over different time periods; (B) Statistically significant differences (P=0.0011, one-way ANOVA) are seen between TCEP mediated N-cleavage in *Mtu*-FL-SufB (i), H-5A (ii), and H-38A (iii). All the experiments were performed in triplicate and error bars represent (±1) SEM. P=Precursor, NC=N-cleavage, LE=Ligated Extein, I=Intein, NE=N-Extein, CC= C-Cleavage.

3.4.2 H-5A and H-38A mutations reduce hydroxylamine (HA) induced N-cleavage

HA is an alpha nucleophile that intercepts between amide-ester equilibrium and induces N-cleavage. It enhances the nucleophilicity of residues that leads to N-cleavage (84, 85). A pseudo-first-order fit for the HA-induced reaction time course with the equation, Y=Y0 +(Plateau-Y0) *(1-exp(-K*x)) was obtained (Figure 5). H-5A and H-38A mutants exhibited about 1.4-fold and 1.5-fold reduction (p=0.0025; one-way ANOVA) in % of N-cleavage, respectively, relative to

Mtu FL-SufB although the K and t1/2 values were comparable [Figure 5C, Table 2 (ii)]. This effect on HA-induced N-cleavage reaction was similar to what is observed in presence of TCEP for the H-5A and H-38A mutations.

3.4.3 H-5A and H-38A mutations do not alter DTT induced N-cleavage

Similar to HA, DTT is also a nucleophile that enhances the nucleophilicity of residues and facilitates N- terminal cleavage reaction (83, 86). N-cleavage efficiency was not noticeably different between H-5A and H-38A mutants and *Mtu*-FL-SufB in presence of DTT (Figure S3 and Table S4). DTT interacts directly with the residues that may increase the flexibility of the active site structure (87), which possibly counteracts the effect of H-5A and H-38A mutations on N-terminal cleavage. The hypothesized role of the histidines at -5 and -38 positions in the N-extein region in direct or indirect Cys1 activation was probed further by MD simulations.

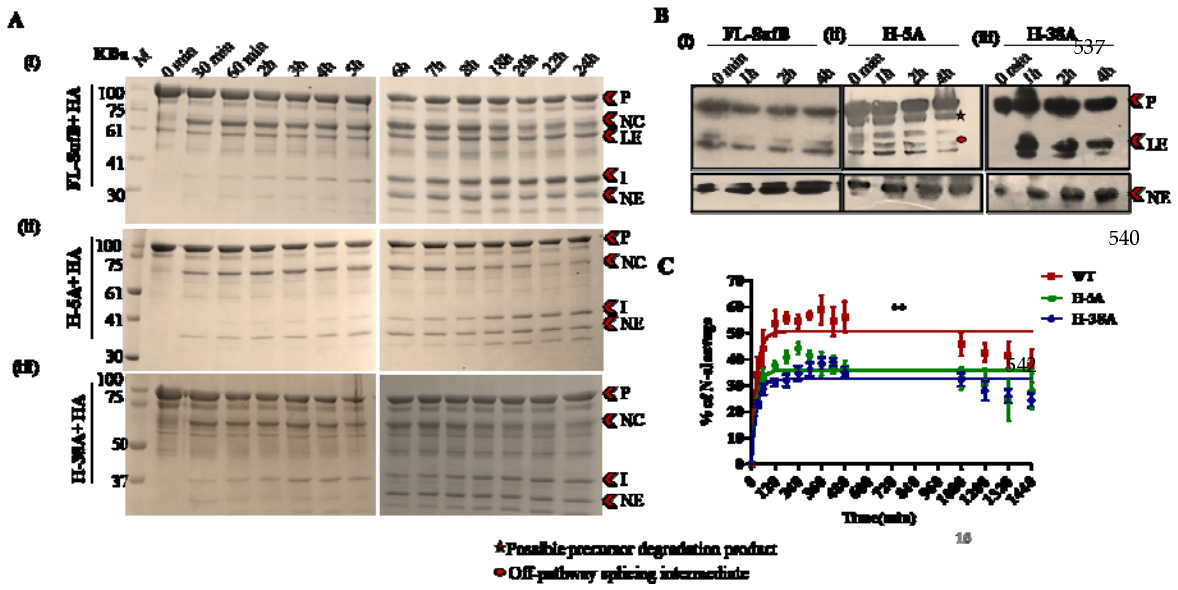

Figure 5. HA mediated N-cleavage in *Mtu* SufB: (A) SDS PAGE analysis of HA induced N-cleavage reactions in (i) *Mtu* FL-SufB precursor, (ii) H-5A, and (iii) H-38A; (B) Western blot analysis of splicing and cleavage products for HA induced N-cleavage reaction in (i) *Mtu* FL-SufB precursor, (ii) H-5A, and (iii) H-38A. NE is blotted separately with higher concentration of

primary antibody; (C) Kinetic analysis of HA induced N-cleavage in WT, H-5A and H-38A mutant proteins suggests statistically significant differences (P= 0.0025; one way ANOVA) in % of N-cleavage. All the experiments were performed in triplicates and error bars represent (±1) SEM. P=Precursor, NC=N-cleavage, LE=Ligated Extein, I=Intein, NE=N-Extein, CC= C-Cleavage product.

Table 2. (i) Comparative analysis of TCEP mediated N-terminal cleavage reaction at 20 °C over 240 mins (data also shown in Figure 4B). (ii) Different kinetic parameters (Ymax, rate constant, and half-life) for HA-induced N-terminal cleavage in FL-SufB precursor, H-5A, and H-38A SufB mutants (data also shown in Figure 5C).

(i)

Time (min)	FL-SufB (% of N-cleavage)	H-5A (% of N-cleavage)	H-38A (% of N-cleavage)
20	28.2±5.5	15.1±0.97	7.42±2
40	36±4.3	17.89±2.7	9.3±2.7
60	30.63±5.1	20.76±3.7	10.2±1.7
80	25.7±5.7	14.9±2.5	12.42±1.9
120	19.8±1.6	8.4±0.7	10.5±2.7
240	16.78±1.5	6.2±0.89	7.07±1.9

(ii)

Kinetic parameters	FL-SufB	H-5A	H-38A
Y_{max}	50.67±1.6	35.72±1.4	32.45±0.94
Rate Constant(K) (min^{-1})	3.7±0.01 $x10^{-2}$	3.9±0.01$x10^{-2}$	3.7±0.009$x10^{-2}$
Half-life($t_{1/2}$)	18.5 min	17.3min	18.2min

3.5 Protein identification

The identity of splicing and cleavage products (P, CC, LE, and NE) for the N-terminal 6X (His) tagged proteins was affirmed via western blot using anti-His antibodies (Figure 3B, 5B, and S3B). SI (C1A/N359A) double mutant SufB was used as a control that yielded just unspliced precursor protein (P) [Figure 3B (iv)]. One additional protein band was noticed above LE and below CC for *Mtu* FL-SufB, H-5A, and H-38A possibly due to a splicing intermediate as an off-pathway product. We also observed a product just below the P band for *Mtu* FL-SufB, SI, H-5A, and H-38A (Figure3B, 5B, and S3B). However, this protein band was missing in cells expressing SufB intein or empty vector pACYC Duet-1 [Figure 3B (iv)]. This indicated that this band corresponded to a SufB precursor degradation product in the cells over-expressing active and inactive *Mtu* FL-SufB precursor.

To further clarify the identity of these different splicing and cleavage products, MALDI-TOF/TOF mass spectrometry (MS) was performed (Table S3) on protein bands cut from the SDS PAGE gel. When the acquired MS and MS/MS spectra were searched against the taxonomy Mycobacterium tuberculosis from NCBInr (88) database, all the splicing products were identified as SufB protein of *Mycobacterium tuberculosis* complex with a statistically significant score (Table S3). A further check against a customized database containing probable splicing and cleavage products of SufB protein of *Mycobacterium tuberculosis* with same parameters for the individual protein band spectra resulted in the identification of matching protein splicing products. Individual protein band identifications with protein score, percent coverage, theoretical molecular weight, and isoelectric pH value are shown in Table S3. Significance is measured from the expectancy-value (with a p-value ≤ 0.05).

Protein fragments of *Mtu* FL-SufB were also found to be within the expected mass range as per retention time (RT) by HPLC (Figure S1).

3.6 Proposed mechanism for the cleavage of N- terminal intein~extein peptide bond

The *in vitro* experimental results suggest that the mechanism of *Mtu* SufB intein cleavage at the N-terminal cleavage site between Gly252 (G-1) and Cys253 (C1) is influenced by two conserved histidines at -5 (248, full-length protein) and -38 (215, full-length protein) positions in the N-extein sequence of the *Mtu* FL-SufB protein. To further probe the basis of this influence, we performed MD simulations on a 3-dimensional (3D) model of the *Mtu* FL-SufB precursor protein (Figure. 6A). This also aided identification of possible critical residues at the SufB intein active site (N- and C-terminal splice junctions) (Figure. 6B and Figure. S7), given their proximity to catalytic residues Cys253 (C1), Cys612 (C+1), and Asn611 (N359).

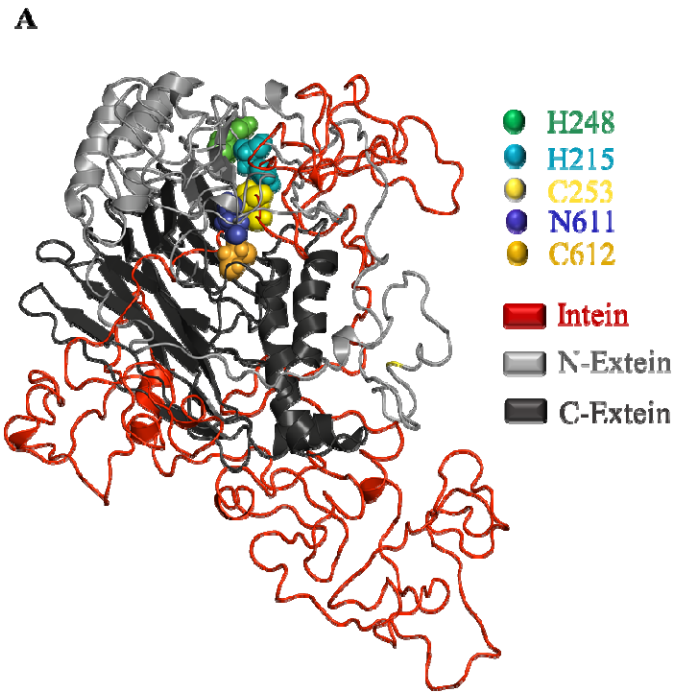

B

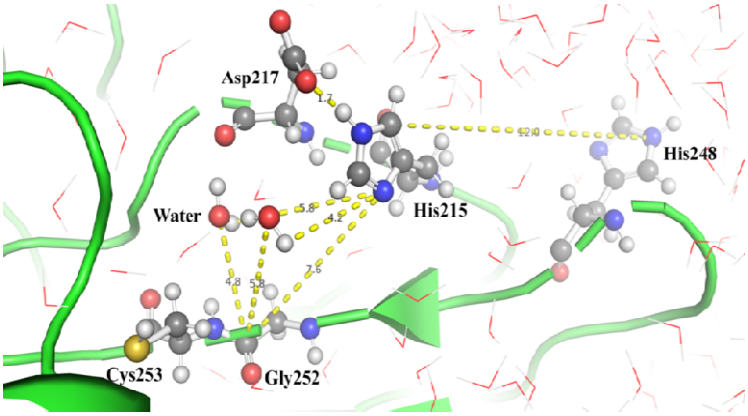
Asp217
His248
Water
His215
Cys253
Gly252

C

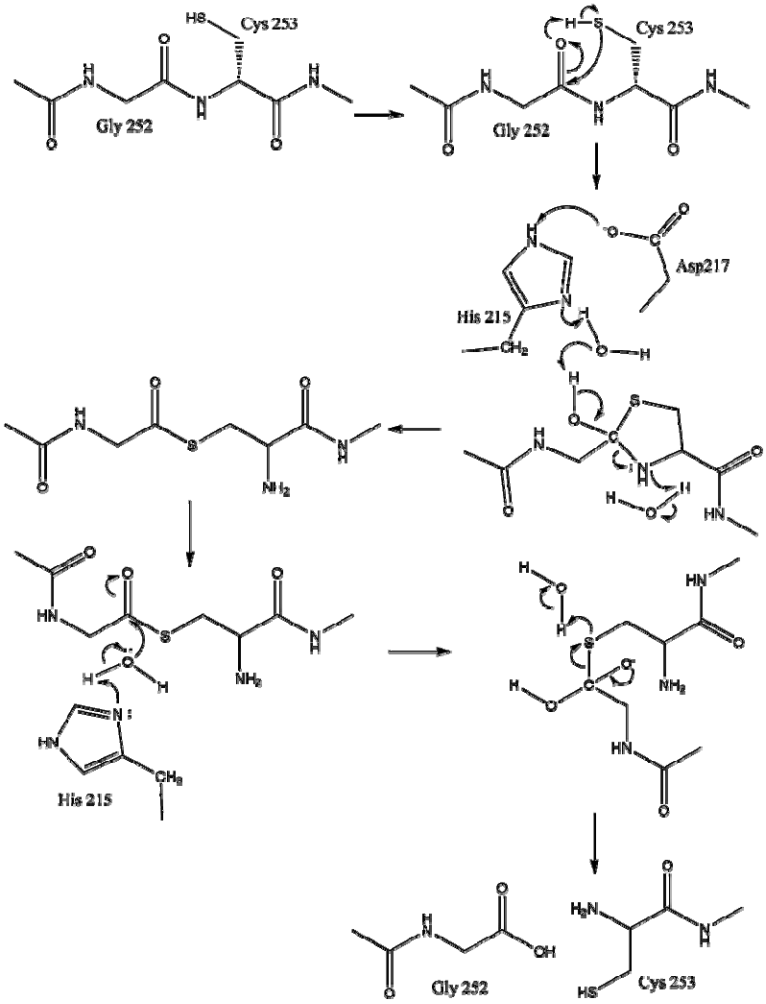
Cys 253
Gly 252
Asp217
His 215
Gly 252
Cys 253

D

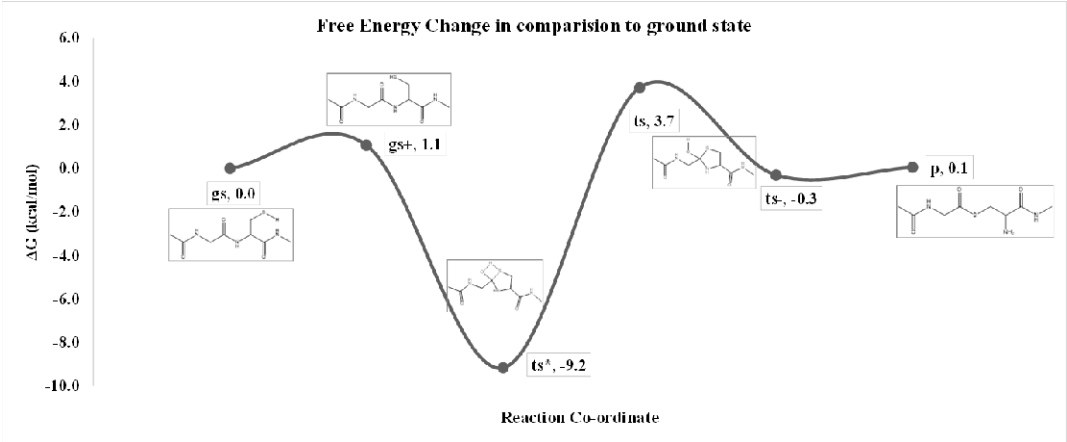

E

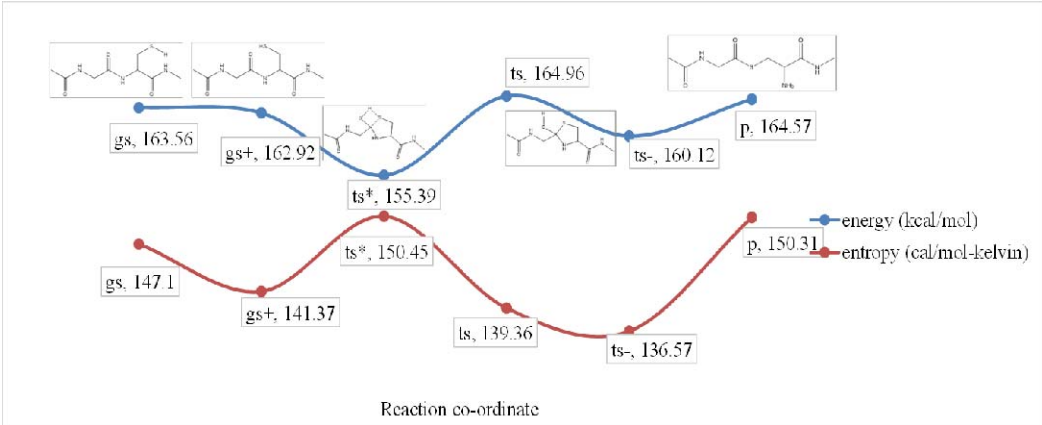

Figure 6. Structural model and proposed mechanism for N-cleavage reaction in *Mtu* FL-SufB precursor. (A) The 3D model of *Mtu* FL-SufB precursor obtained in explicit solvent. Different domains and conserved catalytic residues are color coded as shown in the legend, (B) Spatial arrangement of the N-terminal active site residues; Cys253 (C1) and Gly252 (G-1) along with His248 (H-5), His215 (H-38) and Asp217 (D-36) at the N-terminal cleavage site, (C) Proposed mechanism for N- terminal cleavage reaction at intein~extein junction, (D) Free energy change, and (E) Energy and entropy of the system during QM calculation of different reaction states of N-cleavage junction from peptide bond to thio-ester bond of *Mtu* FL-SufB precursor protein. gs = ground state, gs+ = conformational transition state, ts*= transition state of proton transfer, ts = tetrahedral intermediate, ts = transition state of proton transfer, p = product.

The composite 3D model of *Mtu* FL-SufB precursor was built based on percent sequence identity with analogous sequences from the SufBCD complex of *Escherichia coli* (40% identity, PDB ID: 5AWF, chain A), PI-SceI; a homing endonuclease with protein splicing activity (45% identity, PDB ID: 1VDE, chain A) and intein homing endonuclease II (22% identity, PDB ID: 2CW7, chain A). This model of *Mtu* FL-SufB lacked secondary structure in the intein region due to low sequence identity to the template, with nearly 13% of amino acids are found to be present in the disallowed region in the Ramachandran plot (Figure S5A). To optimize this structure further, we carried out molecular dynamics (MD) simulations of the model in explicit solvent for a duration of 100ns. Based on parameters such as solvent accessible surface area (SASA) (Figure. S4B) and root mean square deviation (RMSD), the structure was found to be equilibrated after 80ns (Figure. S4A). The equilibrated *Mtu* FL-SufB structure was found to have only ~1% amino acids in the disallowed region of the Ramachandran plot (Figure. S5B). We found that the longer side chain amino acids in the disallowed region of the Ramachandran plot were mostly solvent-exposed. The ProSAweb score of the model before and after the 100 ns MD simulations is shown in Figure. S5C and D.

The simulations were also analyzed for the role of specific residues, especially His248 (H-5), which is near the N- and C- cleavage sites. The comparison between 20 ns duration simulations for the *Mtu* FL-SufB precursor and H-5A mutant for RMSD and Root Mean Square Fluctuation (RMSF) parameters is shown in Figure. S6A and B. It was observed that His248 (H-5) attracts His215 (H-38) towards the active site Gly252 (Gly-1), which could facilitate the *Mtu* SufB N-cleavage reaction. Although His-5 is closer to the active site compared to His-38) in the primary sequence, His-38 is closer to the active site in the 3D model. Specifically, the shortest distance

between His-38 and Gly-1 was observed to be 6.8 Å, which is similar to distances observed between catalytic residues in other inteins (12, 39).

Similarly, His610 (His358), Asn 611 (His359), and Cys612 (Cys+1) were located near the C-cleavage site in the *Mtu* FL-SufB MD simulations (Figure S7). The distance between Asn611 (N359) and Cys612 (C+1) was found to be 5.5 ± 0.1 Å and the distance between Asn611 (N359) and His610 (H358) was 4.3 ± 0.3 Å (Table S5). This proximity suggests that the C-cleavage reaction may be facilitated by interactions between these three amino acids, but further analysis of this reaction step is outside the scope of the present study.

Coordination between N-terminal intein~extein splice junction residues Gly252 (Gly-1), Cys253 (Cys1), and His215 (His-38) and His248 (His-5) likely propels *Mtu* SufB N-terminal cleavage. Quantum mechanical (QM) calculations were used to obtain energetics of this N-cleavage reaction as done before for intein cleavage of the *Mtu* RecA intein (23). After the optimized structures of the reactants and the products for each step were obtained, they were used as the initial and final states respectively. Frequency analyses helped identify the stationary points of the intermediates (only real frequencies) and the saddle points of the transition states (one imaginary frequency). The reaction energy barrier was obtained from the energy difference between the transition state and reactant state with the zero-point correction. A postulated schematic for the cleavage reaction, analogous to the canonical intein splicing mechanism (89), is shown in Figure 6C. All stationary states were confirmed by means of vibrational frequency analysis, and the Gibbs free energy at physiological temperature was calculated for all stationary points, including the zero-point energy, the entropy, and the thermal energy (all at 298.15K) at the B3LYP/6-31G (d) (Figure 6D, 6E).

4. DISCUSSION

4.1. Mtu SufB likely follows a canonical intein splicing mechanism

Being an essential component of the mycobacterial SUF system, the SufB protein is well conserved in mycobacteria, bacteria, and archaea. Intein-carrying SufB proteins are found in different mycobacterial species, although the intein insertion points vary in some species (Figure 2) (54). Cladogram analysis suggest some divergence in *M. leprae*, *M. lepromatosis*, *M. xenopi*, *M. triplex* and Ferroplasma in the extein sequences and intein insertion sites, which suggests intein-extein co-evolution and independent intein transfer in different species and kingdoms. Domain analysis of the *Mtu* FL-SufB precursor (846 aa) clearly demarcates the intein and extein structural regions (Figure 1, Table S2), with the *Mtu* SufB intein (359 residues) containing an intact endonuclease domain. Catalytic residues critical for classic intein splicing pathways like Cys1 (Block A), Cys+1 (Block G), penultimate His (Block G), and terminal Asn (Block G) are conserved in different mycobacterial species including *Mtu*. The *Mtu* SufB intein also contains the conserved Block B His67 that is known to catalyze the first N-S acyl shift by destabilizing the scissile peptide bond. In vitro refolding of *Mtu* SufB precursor gives splicing and cleavage products that also concur with the roles of these conserved residues. All these observations suggest that *Mtu* FL-SufB undergoes a canonical (classic) cis-splicing autoprocessing mechanism to form the functional ligated extein protein (Figure 1).

4.2. A distinct N-terminal cleavage mechanism regulated by conserved H-5 and H-38

Sequence analysis detected two highly conserved His residues in the N-extein sequence of *Mtu* SufB protein; His-38 and His-5 located in all SufB proteins where SUF constitutes the exclusive pathway for [Fe-S] cluster generation irrespective of genus and kingdoms (Figure 2A, B).

Catalytic residues such as Cys1, Cys+1, and terminal Asn directly participate in intein splicing by promoting sequential nucleophilic displacement reactions or by rearrangement of bonds near splice junctions. Non-catalytic residues assist indirectly via activation of active site residues and stabilization of various intermediate structure(s). Conserved His residues within intein sequence are known to play important roles during protein splicing as well. Block B His accelerates N-S acyl shift and cleavage of N-terminal intein~extein peptide bond whereas F- and G-Block His are crucial in the coordination of terminal Asn cyclization and cleavage of C-terminal splice site.

Splicing assays and kinetic analysis on *Mtu* FL-SufB precursor and mutant proteins suggests a mechanism where His-5 and His-38 coordinate to facilitate N-cleavage reaction via activation of catalytic Cys1 [Figure 3, 4, and 5]. Both H-5A and H-38A mutants exhibit a sluggish splicing reaction relative to FL- SufB protein under optimum experimental conditions (Table 1). N-cleavage reaction kinetic analysis shows that H-5A and H-38A mutations reduce N-cleavage efficiency in presence of TCEP and HA (Table 2 (i) and (ii), Figure 4 and 5), but DTT-induced thiolysis is unaffected (Figure S3). This may be explained by DTT being a stronger nucleophile that exhibits a more efficient thiolysis and di-sulfide reduction. H-5 and H-38 therefore seem to assist *Mtu* SufB N-cleavage in conjunction with other active site residues.

To further ascertain the roles of these conserved N-extein histidines, a 3D model of the *Mtu* FL-SufB precursor was built by homology modeling. Explicit solvent MD simulations were performed to optimize and equilibrate the model. H-38 was observed to be localized closer to the active site in the optimized model, which suggests that H-5 and H-38 act in a concerted manner to facilitate *Mtu* SufB N-cleavage. Other active site residues such as Gly-1 and Cys1 also seem to be involved. QM/MM calculations using equilibrated structures from the MD simulations provide a quantitative characterization of the energetics of the N-cleavage reaction.

Taken together, these results support the following postulated mechanism for *Mtu* SufB N-cleavage reaction, which is shown as a schematic in Figure 6C. The polarized thiol group of Cys1 approaches the peptidyl C=O, with this transition state being enthalpically favored by an interaction between the thiol H and the peptidyl O atom. The electron density decreases in the C, S, and H atoms while increasing in the O atom. With the imaginary vibrational frequency displacement vector of C=O being towards the thiol, the C and S atoms come closer to form a C-S bond. The proton migration from S to O is highly favored energetically and entropically with a free energy change of -9.2 kcal/mol, which agrees with earlier results (90, 91).The sp2 hybridized peptide carbon becomes sp3 hybridized forming a tetrahedral transition state with a 2-hydroxy thiazolidine ring. This annihilates the peptide resonance to increase the free energy by +3.7 kcal/mol. To regain the sp2 hybridization and resonance stabilization, the 2-hydroxy group expels proton to the environment. In a tetrahedral state, S and N atoms have a Mulliken charge of +0.05 and -0.55. The N atom of the thiazolidine ring accepts a proton from the environment become neutral and forms a thioester intermediate (90, 92). The conversion of a peptide bond to a thioester bond is energetically equivalent at the start as well as the end of the reaction which suggests this process is entropy-driven. The thioester could be hydrolyzed by the imidazole side chain of His-38 mediated by water. Such base catalyzed thioester hydrolysis in an aqueous environment is well known (93). The least distance between His-38 and His-5 in MD simulations is about 6.8 Å suggesting an interaction between these two residues to aid catalysis (12, 19).

Asp-36 could exchange a proton with the His-38. The distance fluctuations between His-38 and His-5 in the MD simulations suggest that the solvent-exposed His-5 could attract His-38 towards the N-cleavage site through water-mediated interactions. His-5 could then facilitate thioester hydrolysis by the attacking species (i.e., hydroxide ion) being generated by His-38.

4.3.Biological significance of conserved histidines in the N-extein sequence of Mtu SufB

[Fe-S] cluster-bearing proteins have important physiological roles in electron transfer, redox regulation, metabolic pathways, cellular responses to external stimuli, and as regulators of gene expression (45). The role of the [Fe-S] cluster is closely associated with the functionality of their bound protein framework. In mycobacteria, the SUF system is the sole pathway for [Fe-S] cluster assembly and repair, especially in response to oxidative stress and iron limiting conditions inside macrophages (46, 52). During such an event, the intracellular Fe supply is either from siderophore chelation or via the metabolism of [Fe-S] clusters associated with specific proteins (45). Thus, iron homeostasis plays a major role in mycobacterial survival and virulence. SufB is a [Fe-S] cluster scaffold protein and a vital component of the functional SUF system, and indirectly promotes mycobacterial persistence under stress(52). Further, SufB has been implicated in mycobacterial iron metabolism(45).

Earlier studies have specified the bonding of Fe in [Fe-S] clusters to mostly cysteines from the protein backbone although there is increasing evidence for other ligands such as histidine, aspartate, arginine, threonine, and tyrosine. The most common alternative ligand for [Fe-S] cluster coordination is histidine that is highly conserved with a role in redox tuning and proton-coupled electron transfer (94). His433(SufB) and His360(SufD) are identified as key protein-ligands for the *de novo* [Fe-S] cluster assembly in *E. coli* (51). It has been shown that these non-cysteine ligands can influence the stability and reactivity of [Fe-S] clusters.

In addition to their possible role in initiating N-cleavage reaction via catalytic Cys1 activation, the conserved His-5 and His-38 residues in the N-extein sequence of *Mtu* SufB may play a role in precursor stabilization. Apart from Cys, His is also an important ligand for metal coordination

(51, 94), and His-5 and His-38 could coordinate to Fe+2/ Fe+3 during [Fe-S] cluster biogenesis. Confirmation of SufB precursor stabilization by coordination of these His residues to [Fe-S] cluster or to Fe^{+2}/ Fe^{+3} would need further studies.

SUF is an exclusive system for biogenesis of Fe-S clusters in many pathogenic organisms such as *Staphylococcus aureus*, *Mycobacterium tuberculosis*, *Plasmodium sp.* and *Toxoplasma*, making it an attractive drug target. For instance, D-Cycloserine is a clinical second-line drug currently used against *M. tuberculosis* and inhibits SufS. SUF is the target system for a polycyclic molecule 882 that has direct interaction with SufC in *S. aureus*(80). The current work may therefore aid development of novel anti-TB drugs targeting SufB function and stability.

Data Availability: All the data are available in the manuscript and supplemental data.

The accession code for the *Mycobacterium tuberculosis* SufB protein used in this study is *P9WFP7 (UniProtKB/Swiss-Prot) and* WP_003407484.1, GI: 397673309 (NCBI protein database).

Confirmation of the identity of different splicing and cleavage products of Mtu FL-SufB protein by mass spectrometric analysis: The data has been deposited to the ProteomeXchange Consortium via PRIDE partner repository with data set identifier PXD015199. The details of the submission are given below.

Project Name: Identification of full length, splicing and cleavage products of SufB protein of SUF-complex of *Mycobacterium tuberculosis*.

Project accession: PXD015199

Reviewer account details:

Username- reviewer73867@ebi.ac.uk

Password: bRxRcbvP

<u>The homology model for the full length Mtu SufB protein has been submitted to Model Archive [Project: ma-x807d]</u>:

Full length *Mtu* SufB protein of SUF complex of *Mycobacterium tuberculosis*; [https://www.modelarchive.org/doi/10.5452/ma-x807d] with the access code: 6pmXRNkvwR.

Funding: Current work is supported by UGC-DAE consortium for scientific research(UGC-DAE-CSR-KC/CRS/15/IOP/08/0562), Kolkata, India. Dr. Sunita Panda (201500000557/IF 140155) was supported by INSPIRE fellowship; INSPIRE Division, DST, Government of India.

Acknowledgements: Our sincere thanks to Prof. Marlene Belfort, Department of Biological Sciences and RNA Institute, University at Albany, Albany, NY, USA, for her valuable comments on the manuscript. The plasmids used in this study are borrowed from Prof. Marlene Belfort's laboratory, University at Albany, Albany, NY, USA. These were engineered by Dr. Sasmita Nayak during her PhD work under the guidance of Prof. Marlene Belfort. We also thank Mr. Sourya Subhra Nasker for providing critical comments on the manuscript. We are thankful to Mr. Rajendra Reddy for technical support at Central Proteomics Facility, Institute of Life sciences, and Bhubaneswar. We also thank Mr. A. Ananda Raman for his timely help in HPC (High Performance computing cluster) to perform computational work at National Institute of Science Education and Research (NISER) Bhubaneswar. Our sincere gratitude to Mrs. Anuradha Das for her help in conducting the HPLC experiment at School of Chemical Sciences, NISER Bhubaneswar and to Dr. Rahul Modak for his help in conducting FPLC at School of Biotechnology, KIIT Deemed to be University.

Conflict of Interest: Authors declare no conflict of interest.

Author contributions: Dr. Sunita Panda: Methodology; Validation; Formal analysis; Investigation; Resources; Data curation; Writing - original draft; Visualization; Funding acquisition. **Ananya Nanda:** Methodology; Validation; Formal analysis; Investigation; Resources; Data curation; Writing - original draft; Writing- Reviewing and Editing; Visualization. **Nilanjan Sahu:** Methodology; Software; Validation; Formal analysis; Writing - original draft. **Deepak Kumar Ojha:** Validation; Formal analysis; Investigation; Resources. **Dr. Biswaranjan Pradhan:** Formal analysis; Resources. **Anjali Rai**: Resources. **Dr. Amol R. Suryawanshi:** Methodology; Validation. **Dr. Nilesh Banavali**: Methodology; Software; Validation; Writing- Reviewing and Editing; Visualization. **Dr. Sasmita Nayak:** Conceptualization; Methodology; Validation; Investigation; Data curation; Writing - original draft; Writing- Reviewing and Editing; Visualization; Supervision; Funding acquisition; Project administration.

References

1. Derbyshire V, Belfort M. Lightning strikes twice: intron–intein coincidence. Proceedings of the National Academy of Sciences. 1998;95(4):1356-7.
2. Lennon CW, Belfort M. Inteins. Current Biology. 2017;27(6):R204-R6.
3. Starokadomskyy P. Protein splicing. Molecular Biology. 2007;41(2):278-93.
4. Novikova O, Topilina N, Belfort M. Enigmatic distribution, evolution, and function of inteins. Journal of Biological Chemistry. 2014;289(21):14490-7.
5. Elleuche S, Pöggeler S. Inteins, valuable genetic elements in molecular biology and biotechnology. Applied Microbiology and Biotechnology. 2010;87(2):479-89.
6. Lennon CW, Stanger M, Banavali NK, Belfort M. Conditional Protein Splicing Switch in Hyperthermophiles through an Intein-Extein Partnership. mBio. 2018;9(1):e02304-17.
7. Lennon CW, Stanger MJ, Belfort M. Mechanism of single-stranded DNA activation of recombinase intein splicing. Biochemistry. 2019;58(31):3335-9.
8. Nanda A, Nasker SS, Mehra A, Panda S, Nayak S. Inteins in Science: Evolution to Application. Microorganisms. 2020;8(12):2004.
9. Panda S, Nanda A, Nasker SS, Sen D, Mehra A, Nayak S. Metal effect on intein splicing: A review. Biochimie. 2021.
10. Lennon CW, Stanger M, Belfort M. Protein splicing of a recombinase intein induced by ssDNA and DNA damage. Genes & development. 2016;30(24):2663-8.

862 11. Kelley DS, Lennon CW, Li Z, Miller MR, Banavali NK, Li H, et al. Mycobacterial DnaB helicase
863 intein as oxidative stress sensor. Nature communications. 2018;9(1):1-15.
864 12. Eryilmaz E, Shah NH, Muir TW, Cowburn D. Structural and dynamical features of inteins and
865 implications on protein splicing. Journal of Biological Chemistry. 2014;289(21):14506-11.
866 13. Gogarten JP, Senejani AG, Zhaxybayeva O, Olendzenski L, Hilario E. Inteins: structure, function,
867 and evolution. Annual Reviews in Microbiology. 2002;56(1):263-87.
868 14. Mills KV, Johnson MA, Perler FB. Protein splicing: how inteins escape from precursor proteins.
869 Journal of Biological Chemistry. 2014;289(21):14498-505.
870 15. Shah NH, Eryilmaz E, Cowburn D, Muir TW. Extein residues play an intimate role in the rate-
871 limiting step of protein trans-splicing. Journal of the American Chemical Society. 2013;135(15):5839-47.
872 16. Pavankumar TL. Inteins: Localized distribution, gene regulation, and protein engineering for
873 biological applications. Microorganisms. 2018;6(1):19.
874 17. Topilina NI, Green CM, Jayachandran P, Kelley DS, Stanger MJ, Piazza CL, et al. SufB intein of
875 Mycobacterium tuberculosis as a sensor for oxidative and nitrosative stresses. Proceedings of the
876 National Academy of Sciences. 2015;112(33):10348-53.
877 18. Topilina NI, Mills KV. Recent advances in in vivo applications of intein-mediated protein splicing.
878 Mobile Dna. 2014;5(1):5.
879 19. Hiraga K, Soga I, Dansereau JT, Pereira B, Derbyshire V, Du Z, et al. Selection and structure of
880 hyperactive inteins: peripheral changes relayed to the catalytic center. Journal of molecular biology.
881 2009;393(5):1106-17.
882 20. Binschik J, Mootz HD. Chemical Bypass of Intein-Catalyzed N–S Acyl Shift in Protein Splicing.
883 Angewandte Chemie International Edition. 2013;52(15):4260-4.
884 21. Du Z, Shemella PT, Liu Y, McCallum SA, Pereira B, Nayak SK, et al. Highly Conserved Histidine
885 Plays a Dual Catalytic Role in Protein Splicing: A p K a Shift Mechanism. Journal of the American Chemical
886 Society. 2009;131(32):11581-9.
887 22. Du Z, Zheng Y, Patterson M, Liu Y, Wang C. p K a Coupling at the Intein Active Site: Implications
888 for the Coordination Mechanism of Protein Splicing with a Conserved Aspartate. Journal of the American
889 Chemical Society. 2011;133(26):10275-82.
890 23. Friedel K, Popp MA, Matern JC, Gazdag EM, Thiel IV, Volkmann G, et al. A functional interplay
891 between intein and extein sequences in protein splicing compensates for the essential block B histidine.
892 Chemical science. 2019;10(1):239-51.
893 24. Mujika J, Lopez X. Unveiling the Catalytic Role of B-Block Histidine in the N–S Acyl Shift Step of
894 Protein Splicing. The Journal of Physical Chemistry B. 2017;121(33):7786-96.
895 25. Pereira B, Shemella PT, Amitai G, Belfort G, Nayak SK, Belfort M. Spontaneous proton transfer to
896 a conserved intein residue determines on-pathway protein splicing. Journal of molecular biology.
897 2011;406(3):430-42.
898 26. Ding Y, Xu M-Q, Ghosh I, Chen X, Ferrandon S, Lesage G, et al. Crystal structure of a mini-intein
899 reveals a conserved catalytic module involved in side chain cyclization of asparagine during protein
900 splicing. Journal of Biological Chemistry. 2003;278(40):39133-42.
901 27. Klabunde T, Sharma S, Telenti A, Jacobs WR, Sacchettini JC. Crystal structure of GyrA intein from
902 Mycobacterium xenopi reveals structural basis of protein splicing. Nature structural biology.
903 1998;5(1):31-6.
904 28. Frutos S, Goger M, Giovani B, Cowburn D, Muir TW. Branched intermediate formation
905 stimulates peptide bond cleavage in protein splicing. Nature chemical biology. 2010;6(7):527-33.
906 29. Mujika JI, Lopez X, Mulholland AJ. Modeling protein splicing: reaction pathway for C-terminal
907 splice and intein scission. The journal of physical chemistry B. 2009;113(16):5607-16.
908 30. Shao Y, PAULUS E. Protein splicing: estimation of the rate of O-N and S-N acyl rearrangements,
909 the last step of the splicing process. The Journal of peptide research. 1997;50(3):193-8.

910 31. Johnson MA, Southworth MW, Herrmann T, Brace L, Perler FB, Wüthrich K. NMR structure of a
911 KlbA intein precursor from Methanococcus jannaschii. Protein Science. 2007;16(7):1316-28.
912 32. Southworth MW, Benner J, Perler FB. An alternative protein splicing mechanism for inteins
913 lacking an N-terminal nucleophile. The EMBO Journal. 2000;19(18):5019-26.
914 33. Brace LE, Southworth MW, Tori K, Cushing ML, Perler F. The Deinococcus radiodurans Snf2
915 intein caught in the act: detection of the Class 3 intein signature Block F branched intermediate. Protein
916 Science. 2010;19(8):1525-33.
917 34. Tori K, Dassa B, Johnson MA, Southworth MW, Brace LE, Ishino Y, et al. Splicing of the
918 mycobacteriophage Bethlehem DnaB intein: identification of a new mechanistic class of inteins that
919 contain an obligate block F nucleophile. Journal of Biological Chemistry. 2010;285(4):2515-26.
920 35. Tori K, Perler FB. Expanding the definition of class 3 inteins and their proposed phage origin.
921 Journal of bacteriology. 2011;193(8):2035-41.
922 36. Amitai G, Callahan BP, Stanger MJ, Belfort G, Belfort M. Modulation of intein activity by its
923 neighboring extein substrates. Proceedings of the National Academy of Sciences. 2009;106(27):11005-
924 10.
925 37. Shemella P, Pereira B, Zhang Y, Van Roey P, Belfort G, Garde S, et al. Mechanism for intein C-
926 terminal cleavage: a proposal from quantum mechanical calculations. Biophysical journal.
927 2007;92(3):847-53.
928 38. Sun P, Ye S, Ferrandon S, Evans TC, Xu M-Q, Rao Z. Crystal structures of an intein from the split
929 dnaE gene of Synechocystis sp. PCC6803 reveal the catalytic model without the penultimate histidine
930 and the mechanism of zinc ion inhibition of protein splicing. Journal of molecular biology.
931 2005;353(5):1093-105.
932 39. Topilina NI, Novikova O, Stanger M, Banavali NK, Belfort M. Post-translational environmental
933 switch of RadA activity by extein–intein interactions in protein splicing. Nucleic acids research.
934 2015;43(13):6631-48.
935 40. Cheriyan M, Pedamallu CS, Tori K, Perler F. Faster protein splicing with the Nostoc punctiforme
936 DnaE intein using non-native extein residues. Journal of Biological Chemistry. 2013;288(9):6202-11.
937 41. Chong S, Williams KS, Wotkowicz C, Xu M-Q. Modulation of protein splicing of the
938 Saccharomyces cerevisiae vacuolar membrane ATPase intein. Journal of Biological Chemistry.
939 1998;273(17):10567-77.
940 42. Oeemig JS, Zhou D, Kajander T, Wlodawer A, Iwaï H. NMR and crystal structures of the
941 Pyrococcus horikoshii RadA intein guide a strategy for engineering a highly efficient and promiscuous
942 intein. Journal of molecular biology. 2012;421(1):85-99.
943 43. Shemella PT, Topilina NI, Soga I, Pereira B, Belfort G, Belfort M, et al. Electronic structure of
944 neighboring extein residue modulates intein C-terminal cleavage activity. Biophysical journal.
945 2011;100(9):2217-25.
946 44. Cheriyan M, Chan S-H, Perler F. Traceless splicing enabled by substrate-induced activation of the
947 Nostoc punctiforme Npu DnaE intein after mutation of a catalytic cysteine to serine. Journal of
948 molecular biology. 2014;426(24):4018-29.
949 45. Huet G, Daffé M, Saves I. Identification of the Mycobacterium tuberculosis SUF machinery as the
950 exclusive mycobacterial system of [Fe-S] cluster assembly: evidence for its implication in the pathogen's
951 survival. Journal of bacteriology. 2005;187(17):6137-46.
952 46. Outten FW. Recent advances in the Suf Fe–S cluster biogenesis pathway: beyond the
953 Proteobacteria. Biochimica et Biophysica Acta (BBA)-Molecular Cell Research. 2015;1853(6):1464-9.
954 47. Lin C-W, McCabe JW, Russell DH, Barondeau DP. Molecular Mechanism of ISC Iron–Sulfur
955 Cluster Biogenesis Revealed by High-Resolution Native Mass Spectrometry. Journal of the American
956 Chemical Society. 2020;142(13):6018-29.

957 48. Mettert EL, Kiley PJ. Fe–S proteins that regulate gene expression. Biochimica et Biophysica Acta
958 (BBA)-Molecular Cell Research. 2015;1853(6):1284-93.
959 49. Novikova O, Jayachandran P, Kelley DS, Morton Z, Merwin S, Topilina NI, et al. Intein clustering
960 suggests functional importance in different domains of life. Molecular biology and evolution.
961 2016;33(3):783-99.
962 50. Outten FW, Djaman O, Storz G. A suf operon requirement for Fe–S cluster assembly during iron
963 starvation in Escherichia coli. Molecular microbiology. 2004;52(3):861-72.
964 51. Yuda E, Tanaka N, Fujishiro T, Yokoyama N, Hirabayashi K, Fukuyama K, et al. Mapping the key
965 residues of SufB and SufD essential for biosynthesis of iron-sulfur clusters. Scientific reports.
966 2017;7(1):9387.
967 52. Huet G, Castaing J-P, Fournier D, Daffé M, Saves I. Protein splicing of SufB is crucial for the
968 functionality of the Mycobacterium tuberculosis SUF machinery. Journal of bacteriology.
969 2006;188(9):3412-4.
970 53. Larking M, Blackshields G, Brown N, Chenna R, McGettigan G, McWilliam H, et al. ClustalW and
971 ClustalX version 2. Bioinformatics. 2007;23(21):2947-8.
972 54. Perler FB. InBase: the intein database. Nucleic acids research. 2002;30(1):383-4.
973 55. Morgenstern B. DIALIGN 2: improvement of the segment-to-segment approach to multiple
974 sequence alignment. Bioinformatics (Oxford, England). 1999;15(3):211-8.
975 56. Kumar S, Stecher G, Li M, Knyaz C, Tamura K. MEGA X: molecular evolutionary genetics analysis
976 across computing platforms. Molecular biology and evolution. 2018;35(6):1547-9.
977 57. Truszkowski J, Goldman N. Maximum likelihood phylogenetic inference is consistent on multiple
978 sequence alignments, with or without gaps. Systematic biology. 2016;65(2):328-33.
979 58. Chan H, Pearson CS, Green CM, Li Z, Zhang J, Belfort G, et al. Exploring intein inhibition by
980 platinum compounds as an antimicrobial strategy. Journal of Biological Chemistry. 2016;291(43):22661-
981 70.
982 59. Gangopadhyay JP, Jiang S-q, Paulus H. An in vitro screening system for protein splicing inhibitors
983 based on green fluorescent protein as an indicator. Analytical chemistry. 2003;75(10):2456-62.
984 60. Mills KV, Lew BM, Jiang S-q, Paulus H. Protein splicing in trans by purified N-and C-terminal
985 fragments of the Mycobacterium tuberculosis RecA intein. Proceedings of the National Academy of
986 Sciences. 1998;95(7):3543-8.
987 61. Mills KV, Paulus H. Reversible inhibition of protein splicing by zinc ion. Journal of Biological
988 Chemistry. 2001;276(14):10832-8.
989 62. Zhang L, Zheng Y, Callahan B, Belfort M, Liu Y. Cisplatin inhibits protein splicing, suggesting
990 inteins as therapeutic targets in mycobacteria. Journal of Biological Chemistry. 2011;286(2):1277-82.
991 63. Yamaguchi H, Miyazaki M. Refolding techniques for recovering biologically active recombinant
992 proteins from inclusion bodies. Biomolecules. 2014;4(1):235-51.
993 64. Shevchenko A, Tomas H, Havli J, Olsen JV, Mann M. In-gel digestion for mass spectrometric
994 characterization of proteins and proteomes. Nature protocols. 2006;1(6):2856-60.
995 65. Saxena R, Singh R. MALDI-TOF MS and CD spectral analysis for identification and structure
996 prediction of a purified, novel, organic solvent stable, fibrinolytic metalloprotease from Bacillus cereus
997 B80. BioMed research international. 2015;2015.
998 66. Suryawanshi AR, Khan SA, Gajbhiye RK, Gurav MY, Khole VV. Differential proteomics leads to
999 identification of domain-specific epididymal sperm proteins. Journal of andrology. 2011;32(3):240-59.
1000 67. Wiederstein M, Sippl MJ. ProSA-web: interactive web service for the recognition of errors in
1001 three-dimensional structures of proteins. Nucleic acids research. 2007;35(suppl_2):W407-W10.
1002 68. Abraham MJ, Murtola T, Schulz R, Páll S, Smith JC, Hess B, et al. GROMACS: High performance
1003 molecular simulations through multi-level parallelism from laptops to supercomputers. SoftwareX.
1004 2015;1:19-25.

1005 69. Kaminski GA, Friesner RA, Tirado-Rives J, Jorgensen WL. Evaluation and reparametrization of the
1006 OPLS-AA force field for proteins via comparison with accurate quantum chemical calculations on
1007 peptides. The Journal of Physical Chemistry B. 2001;105(28):6474-87.
1008 70. Berendsen H, Grigera J, Straatsma T. The missing term in effective pair potentials. Journal of
1009 Physical Chemistry. 1987;91(24):6269-71.
1010 71. Kusalik PG, Svishchev IM. The spatial structure in liquid water. Science. 1994;265(5176):1219-21.
1011 72. Fletcher R, Powell MJ. A rapidly convergent descent method for minimization. The computer
1012 journal. 1963;6(2):163-8.
1013 73. Grubmüller H, Heller H, Windemuth A, Schulten K. Generalized Verlet algorithm for efficient
1014 molecular dynamics simulations with long-range interactions. Molecular Simulation. 1991;6(1-3):121-42.
1015 74. Barnes J, Hut P. A hierarchical O (N log N) force-calculation algorithm. nature.
1016 1986;324(6096):446.
1017 75. Hess B, Bekker H, Berendsen HJ, Fraaije JG. LINCS: a linear constraint solver for molecular
1018 simulations. Journal of computational chemistry. 1997;18(12):1463-72.
1019 76. Darden T, York D, Pedersen L. Particle mesh Ewald: An N· log (N) method for Ewald sums in large
1020 systems. The Journal of chemical physics. 1993;98(12):10089-92.
1021 77. Perler FB. Protein splicing of inteins and hedgehog autoproteolysis: structure, function, and
1022 evolution. Cell. 1998;92(1):1-4.
1023 78. Pearson WR. An introduction to sequence similarity ("homology") searching. Current protocols
1024 in bioinformatics. 2013;42(1):3.1. -3.1. 8.
1025 79. Albrecht AG, Netz DJ, Miethke M, Pierik AJ, Burghaus O, Peuckert F, et al. SufU is an essential
1026 iron-sulfur cluster scaffold protein in Bacillus subtilis. Journal of bacteriology. 2010;192(6):1643-51.
1027 80. Pérard J, de Choudens SO. Iron–sulfur clusters biogenesis by the SUF machinery: close to the
1028 molecular mechanism understanding. JBIC Journal of Biological Inorganic Chemistry. 2018;23(4):581-96.
1029 81. Zhang B, Rapolu M, Liang Z, Han Z, Williams PG, Su WW. A dual-intein autoprocessing domain
1030 that directs synchronized protein co-expression in both prokaryotes and eukaryotes. Scientific reports.
1031 2015;5:8541.
1032 82. Kirby AJ, Souza BS, Medeiros M, Priebe JP, Manfredi AM, Nome F. Hydroxylamine as an oxygen
1033 nucleophile. Chemical evidence from its reaction with a phosphate triester. Chemical Communications.
1034 2008(37):4428-9.
1035 83. Bachmann A-L, Mootz HD. An unprecedented combination of serine and cysteine nucleophiles in
1036 a split intein with an atypical split site. Journal of Biological Chemistry. 2015;290(48):28792-804.
1037 84. Simanenko YS, Popov A, Prokop'eva T, Savelova V, Belousova I. Hydroxylamine anion—an
1038 effective α-nucleophile in acyl transfer reactions. Theoretical and Experimental Chemistry.
1039 1994;30(2):61-4.
1040 85. Xu M-Q, Perler FB. The mechanism of protein splicing and its modulation by mutation. The
1041 EMBO journal. 1996;15(19):5146-53.
1042 86. Volkmann G, Sun W, Liu XQ. Controllable protein cleavages through intein fragment
1043 complementation. Protein Science. 2009;18(11):2393-402.
1044 87. Alliegro MC. Effects of Dithiothreitol on Protein Activity Unrelated to Thiol–Disulfide Exchange:
1045 For Consideration in the Analysis of Protein Function with Cleland's Reagent. Analytical biochemistry.
1046 2000;282(1):102-6.
1047 88. Pruitt KD, Tatusova T, Maglott DR. NCBI Reference Sequence (RefSeq): a curated non-redundant
1048 sequence database of genomes, transcripts and proteins. Nucleic acids research.
1049 2005;33(suppl_1):D501-D4.
1050 89. Chong S, Shao Y, Paulus H, Benner J, Perler FB, Xu M-Q. Protein Splicing Involving the
1051 Saccharomyces cerevisiae VMA Intein The steps in the splicing pathway, side reactions leading to

1052 protein cleavage, and establishment of an in vitro splicing system. Journal of Biological Chemistry.
1053 1996;271(36):22159-68.
1054 90. Burke HM, McSweeney L, Scanlan EM. Exploring chemoselective S-to-N acyl transfer reactions in
1055 synthesis and chemical biology. Nature communications. 2017;8(1):1-16.
1056 91. Devaraj NK, Perrin CL. Approach control. Stereoelectronic origin of geometric constraints on N-
1057 to-S and N-to-O acyl shifts in peptides. Chemical science. 2018;9(7):1789-94.
1058 92. Monbaliu J-CM, Dive G, Stevens CV, Katritzky AR. Governing parameters of long-range
1059 intramolecular S-to-N acyl transfers within (S)-acyl isopeptides. Journal of chemical theory and
1060 computation. 2013;9(2):927-34.
1061 93. Kirsch JF, Jencks WP. Base catalysis of imidazole catalysis of ester hydrolysis. Journal of the
1062 American Chemical Society. 1964;86(5):833-7.
1063 94. Bak DW, Elliott SJ. Alternative FeS cluster ligands: tuning redox potentials and chemistry.
1064 Current opinion in chemical biology. 2014;19:50-8.

1065

1066

1067

1068

1069

1070

1071

1072

1073

1074

1075

1076

1077

1078

1079

1080

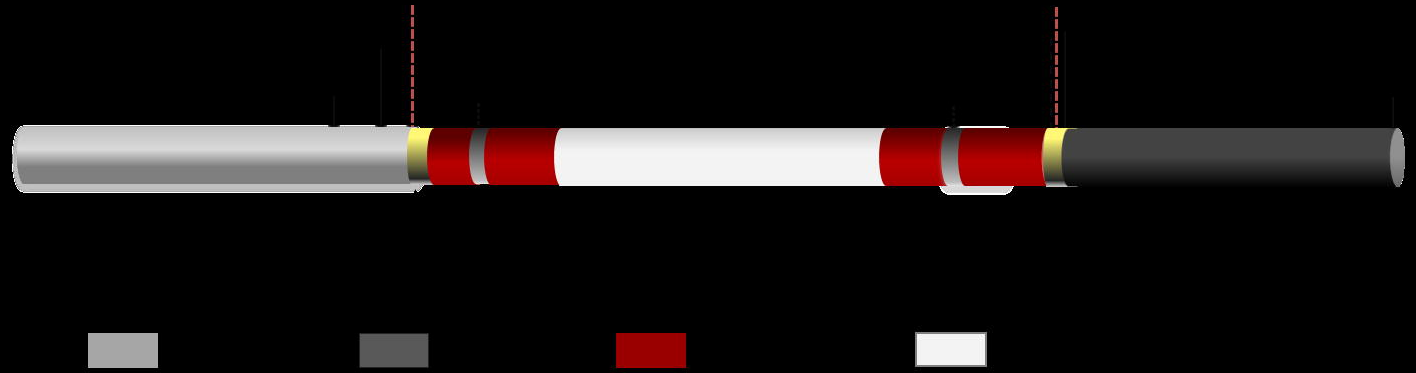

```
Mtu SufB    CLPAGELITTADG ANAFSVTAEHPLLA PVYNLDVENPDSYL YGFAVHNC
Mbo SufB    CLPAGELITTADG ANAFSVTAEHPLLA PVYNLDVENPDSYL YGFAVHNC
Maf SufB    CLPAGELITTADG ANAFSVTAEHPLLA PVYNLDVENPDSYL YGFAVHNC
Mtu RecA    CLAEGTRIFDPVT GAIVWATPDHKVLT RTFDLEVEELHTLV EGVVVHNC
Npu DnaE    CLSYETEILTVEY GSVIRATSDHRFLT NVYDIGVERDHNFA NGFIASNC
Npu DnaB    CLAGDSLVTLVDS GRKIRATGNHKFLT EVFDLTVPGLHNFV NNIIVHNS
Ssp DnaE    CLSFGTEILTVEY GSVIRATSDHRFLT RIFDiGLPQDHNFL NGAIAANC
Sce  VMA    CFAKGTNVLMADG LLKFTCNATHELVV YGITLSDDSDHQFL NQVVVHNC
```

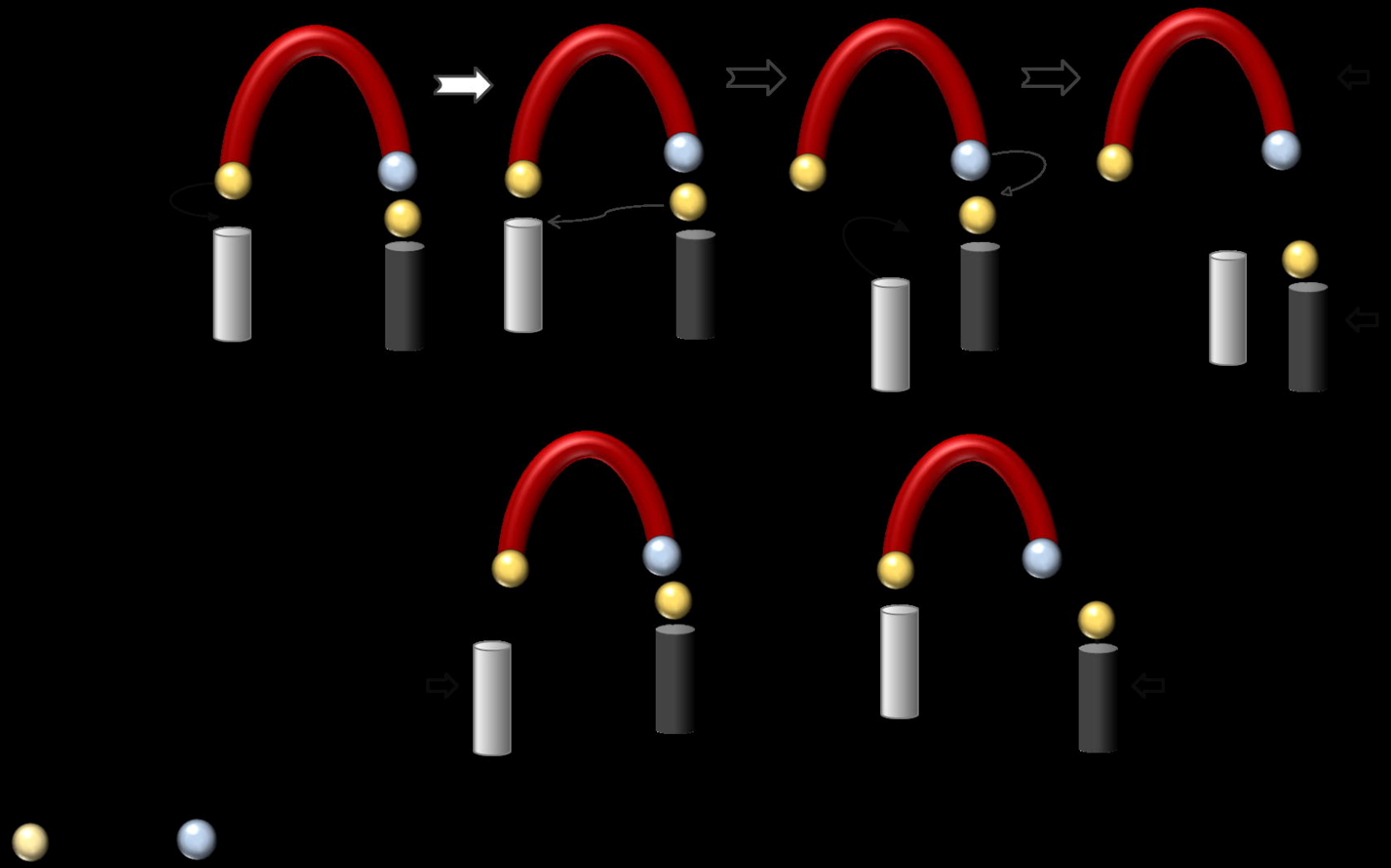

```
M.tuberculosis (206)   ---------- ---------- ----SFIYVP PGVHVDIPLQ AYFRINTENM (231)
M.microti      (206)   ---------- ---------- ----SFIYVP PGVHVDIPLQ AYFRINTENM (231)
M.africanum    (206)   ---------- ---------- ----SFIYVP PGVHVDIPLQ AYFRINTENM (231)
M.bovis        (206)   ---------- ---------- ----SFIYVP PGVHVDIPLQ AYFRINTENM (231)
M.Bourgelatii  (199)   ---------- ---------- ----SFIYVP PGVHVDIPLQ AYFRINTENM (224)
M.Kansasii     (199)   ---------- ---------- ----SFIYVP PGVHVDIPLQ AYFRINTENM (224)
M.orygis       (206)   ---------- ---------- ----SFIYVP PGVHVDIPLQ AYFRINTENM (231)
M.gastri_W     (199)   ---------- ---------- ----SFIYVP PGVHVDIPLQ AYFRINTENM (224)
M.gastri_p     (453)   ---------- ---------- ----SFIYVP PGVHVDIPLQ AYFRINXENM (224)
M.canettii     (211)   ---------- ---------- ----SFIYVP PGVHVDIPLQ AYFRINTENM (236)
M.caprae       (206)   ---------- ---------- ----SFIYVP PGVHVDIPLQ AYFRINTENM (231)
M.Pinnipeddii  (206)   ---------- ---------- ----SFIYVP PGVHVDIPLQ AYFRINTENM (231)
M.xenopi       (578)   ---------- ---------- ----SFIYVP PGVHVEIPLQ AYFRINTENM (603)
M.triplex      (577)   ---------- ---------- ----SFIYVP PGVHVDIPLQ AYFRINTENM (602)
M.leprae       (564)   EKPTYDIQVV GLENFVANGI VAHNSFIYVP PGVHVDIPLQ AYFRINTENM (613)
M.lepromatosis (563)   EKPTYDIQVV GLENFVANGI VAHNSFIYVP PGVHVDIPLQ AYFRINTENM (612)
Ferroplasma    (196)   ---------- ---------- ----SFLYVP KNVTIDMPLQ TYFRMNGEQS (221)

M.tuberculosis (232)   GQFERTLIIA DEGSYVHYVE GGLPAGELIT TADGDLRPIE SIRVGDFVTG (281)
M.microti      (232)   GQFERTLIIA DEGSYVHYVE GGLPAGELIT TADGDLRPIE SIRVGDFVTG (281)
M.africanum    (232)   GQFERTLIIA DEGSYVHYVE GGLPAGELIT TADGDLRPIE SIRVGDFVTG (281)
M.bovis        (232)   GQFERTLIIA DEGSYVHYVE GGLPAGELIT TADGDLRPIE SIRVGDFVTG (281)
M.Bourgelatii  (225)   GQFERTLIIA DEGSYVHYVE GGLPAGELIT TADGDLRPIE SIQVGDYVTG (274)
M.Kansasii     (225)   GQFERTLIIA DEGSYVHYVE GGVPAGELIT TADGDLRPIE SIRVGDYVSS (274)
M.orygis       (232)   GQFERTLIIA DEGSYVHYVE GGLPAGELIT TADGDLRPIE SIRVGDFVTG (281)
M.gastri_W     (225)   GQFERTLIIA DEGSYVHYVE GGLPAGELIT TADGDLRPIE SIRVGDYVTG (274)
M.gastri_p     (479)   GQFERTLIIV GENAYVTYVE G--------- ---------- ---------- (499)
M.canettii     (237)   GQFERTLIIA DEGSYVHYVE GGLPAGELIT TADGDLRPIE SIRVGDFVTG (286)
M.caprae       (232)   GQFERTLIIA DEGSYVHYVE GGLPAGELIT TADGDLRPIE SIRVGDFVTG (281)
M.Pinnipeddi   (232)   GQFERTLIIA DEGSYVHYVE GGLPAGELIT TADGDLRPIE SIRVGDFVTG (281)
M.xenopi       (604)   GQFERTLIIV DENAYVHYVE G--------- ---------- ---------- (624)
M.triplex      (603)   GQFERTLIIV DEGAYVHYVE G--------- ---------- ---------- (623)
M.leprae       (614)   GQFERTLIIA DTGSYVHYVE G--------- ---------- ---------- (634)
M.lepromatosis (613)   GQFERTLIIA DEGSYVHYVE G--------- ---------- ---------- (633)
Ferroplasma    (222)   GQFEHTIVVA DEGAKVHYIE GGLPEDELIS QGDkfv-PIN ELLTDDSVVS (270)
```

```
M.tuberculosis    (181) EYFGTVIPAGDNKFSALNTAVWSGGSFIYVPPGVHVDIPLQAYFRINTENMGQFERTLII(240)
M.marinum         (174) QYFGTVIPAGDNKFSALNTAVWSGGSFIYVPPGVHVDIPLQAYFRINTENMGQFERTLII(245)
M.fortuitum       (181) KYFGTVIPAGDNKFSALNTAVWSGGSFIYVPPGVHVDIPLQAYFRINTENMGQFERTLII(251)
M.smegmatis       (171) QYFGTVIPAGDNKFSALNTAVWSGGSFIYVPPGVHVDIPLQAYFRINTENMGQFERTLII(241)
M.shigaense       (175) QYFGSVIPAGDNKFSALNTAVWSGGSFIYVPPGVHVDIPLQAYFRINTENMGQFERTLII(245)
S.aureus          (159) KYFASVVPAADNKFAALNSAVWSGGSFIYVPKNIKLDTPLQAYFRINSENMGQFERTLII(229)
B.subtilis        (159) EHWAKVIPPTDNKFAALNSAVWSGGSFIYVPKGVKVETPLQAYFRINSENMGQFERTLII(229)

M.tuberculosis    (241) ADEGSYVHYVEGCLPAGELITTADGDLRPIESIRVGDFVTGHDGRPHRVTAVQVRDLDGE(290)
M.marinum         (235) ADEGSYVHYVEG------------------------------------------------(246)
M.fortuitum       (241) ADEGSYVHYVEG------------------------------------------------(252)
M.smegmatis       (231) VDEGAYVHYVEG------------------------------------------------(242)
M.shigaense       (235) VDEGAYVHYVEG------------------------------------------------(246)
S.aureus          (219) ADEGASVHYVEG------------------------------------------------(230)
B.subtilis        (219) VDEEASVHYVEG------------------------------------------------(230)
```

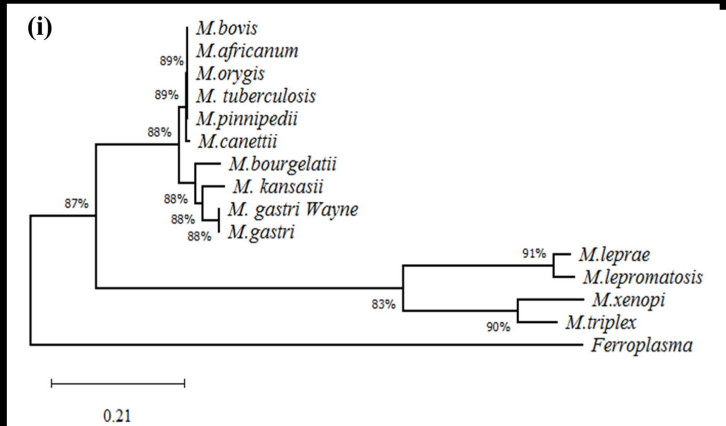
(i)
M.bovis
M.africanum
M.orygis
M. tuberculosis
M.pinnipedii
M.canettii
M.bourgelatii
M. kansasii
M. gastri Wayne
M.gastri
M.leprae
M.lepromatosis
M.xenopi
M.triplex
Ferroplasma
89%
89%
88%
87%
88%
88%
88%
91%
83%
90%
0.21

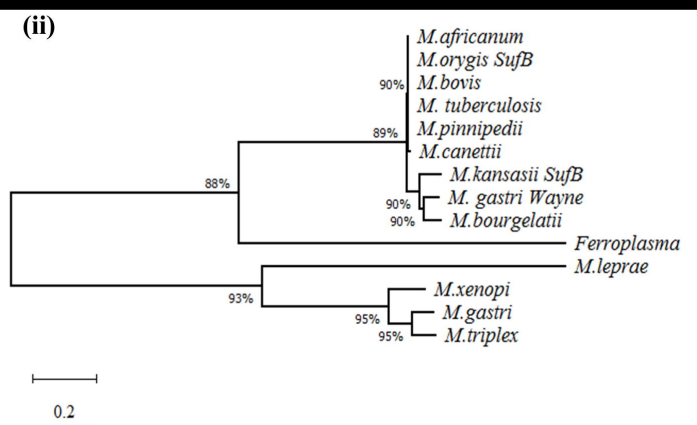
(ii)
M.africanum
M.orygis SufB
M.bovis
M. tuberculosis
M.pinnipedii
M.canettii
M.kansasii SufB
M. gastri Wayne
M.bourgelatii
Ferroplasma
M.leprae
M.xenopi
M.gastri
M.triplex
90%
89%
88%
90%
90%
93%
95%
95%
0.2

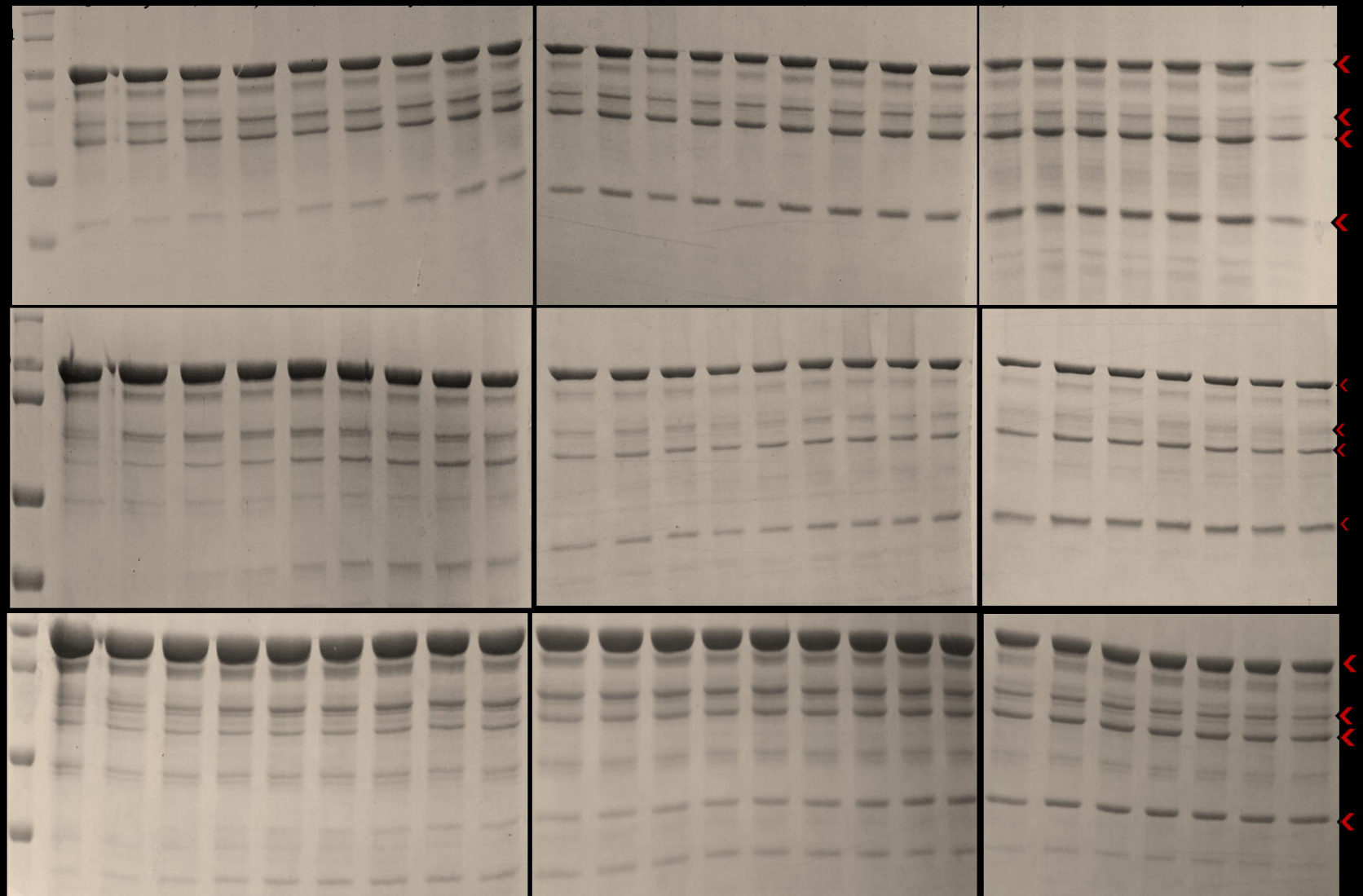

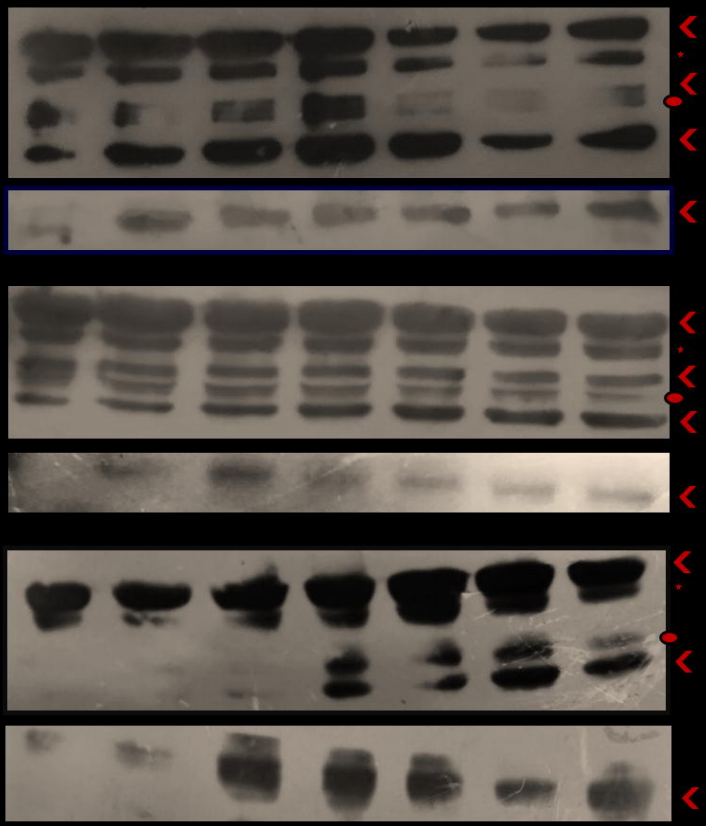

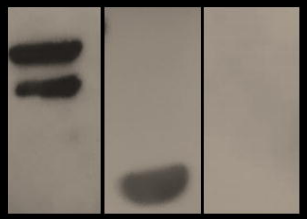

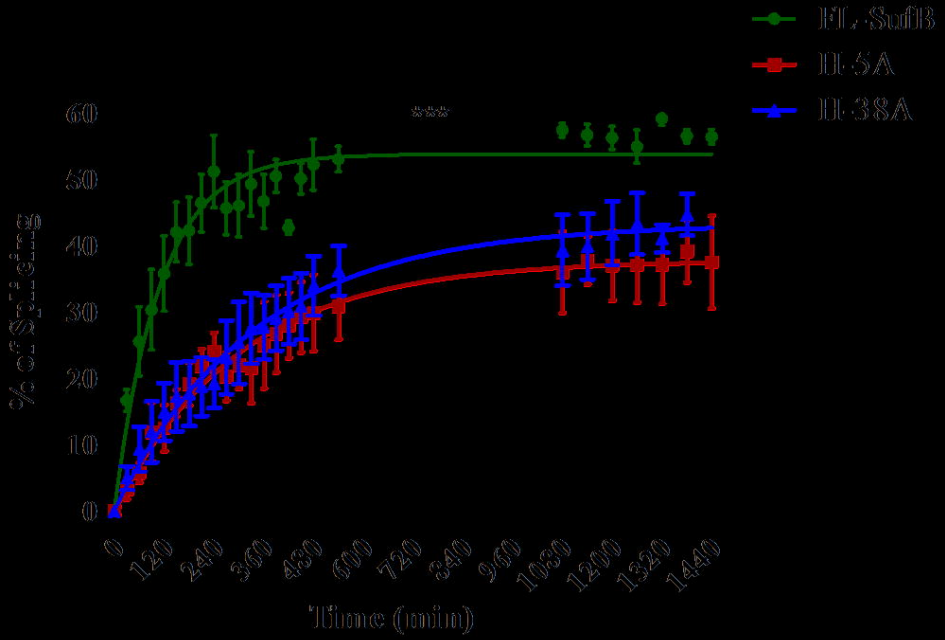
FL-SufB
II-5A
II-38A
***
% of Stringing
0
10
20
30
40
50
60
0
120
240
360
480
600
720
840
960
1080
1200
1320
1440
Time (min)

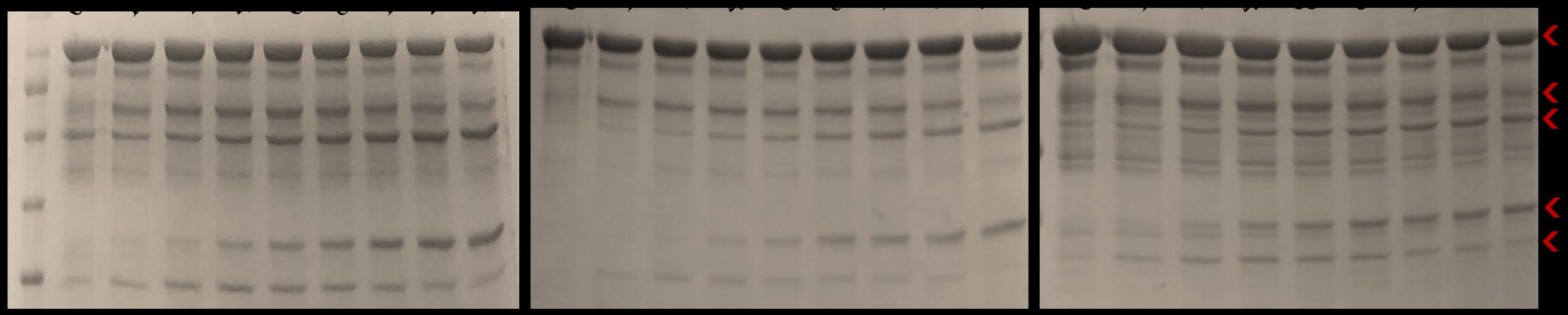

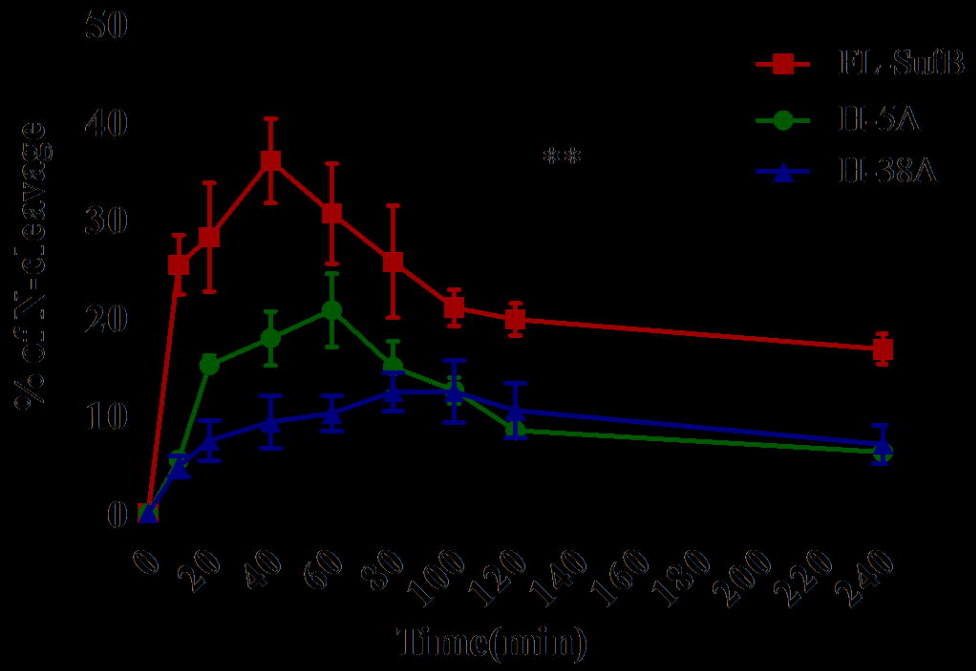
50
40
30
20
10
0
% of N-cleavage
**
FL-SufB
DI-5A
DI-38A
0
20
40
60
80
100
120
140
160
180
200
220
240
Time(min)

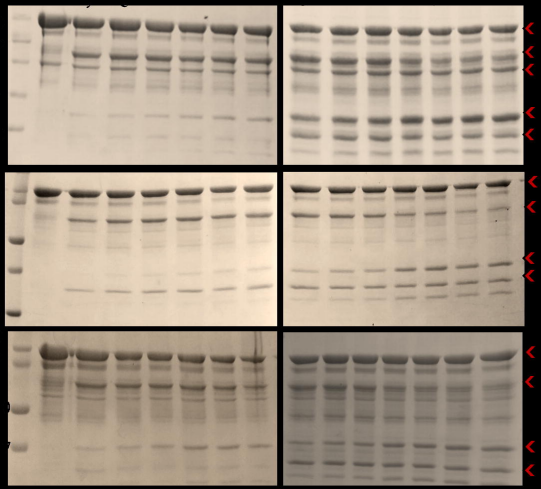

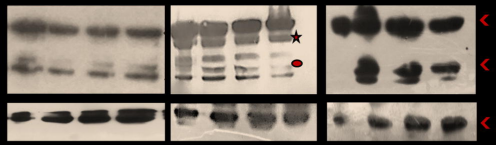

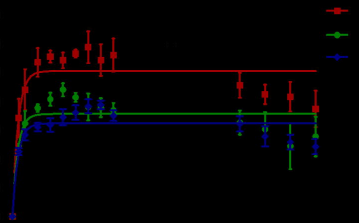

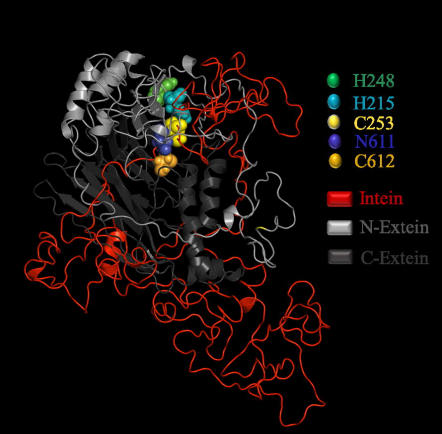
H248
H215
C253
N611
C612
Intein
N-Extein
C-Extein

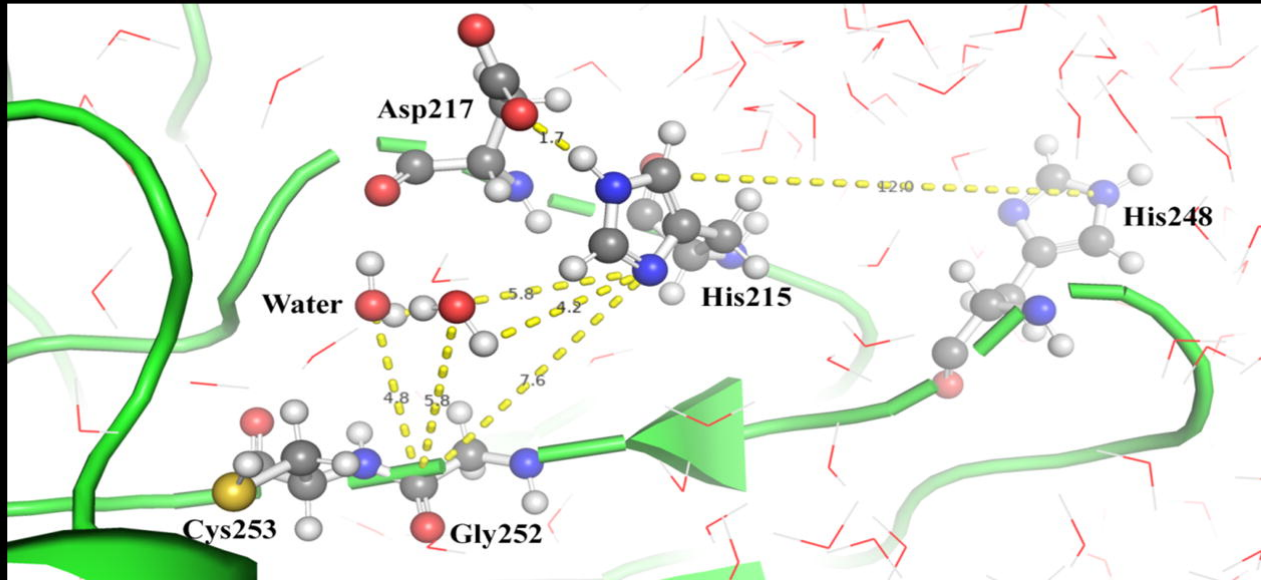
Asp217
1.7
12.0
His248
Water
5.8
4.2
His215
4.8
5.8
7.6
Cys253
Gly252

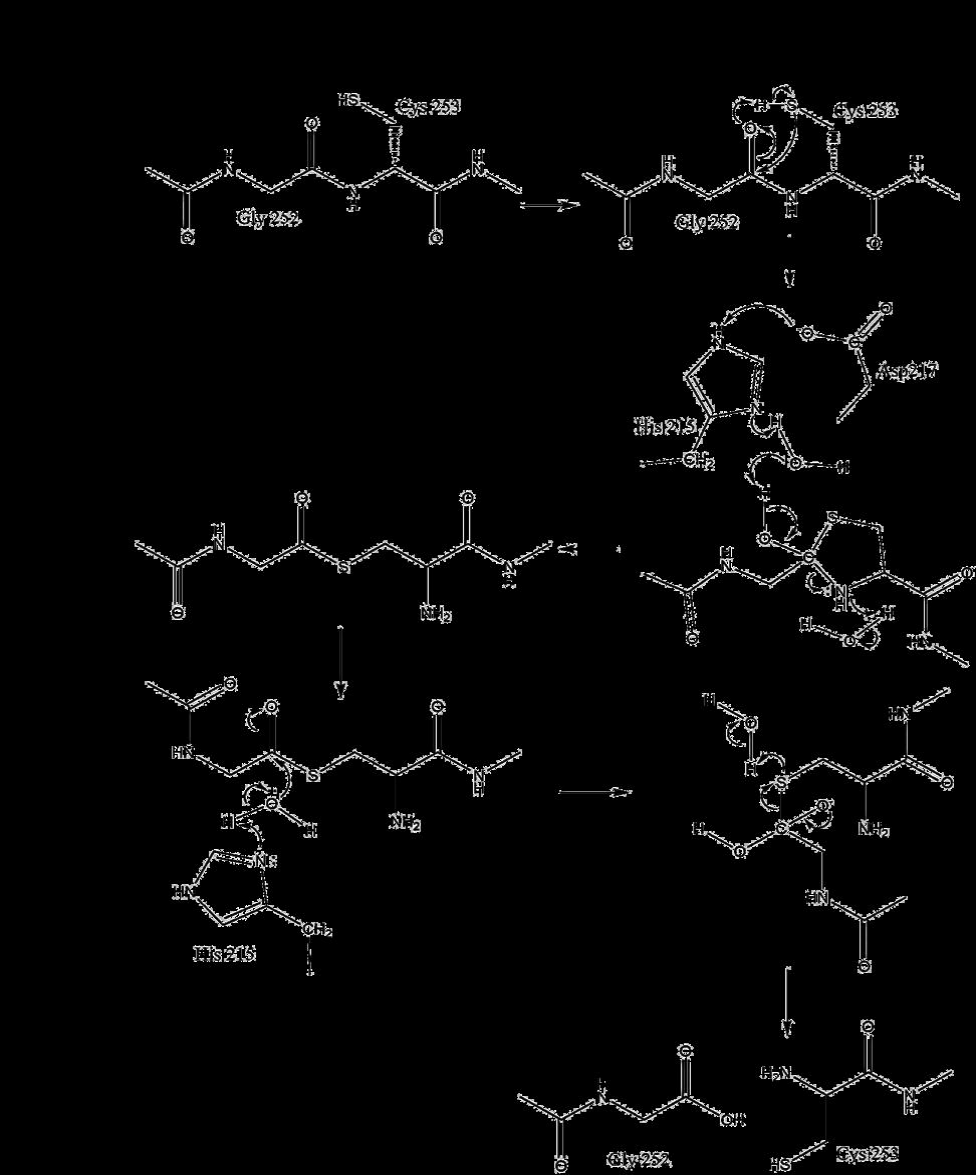
Cys253
Gly252
Cys253
Gly252
Asp217
His215
His215
Gly252
Cys253

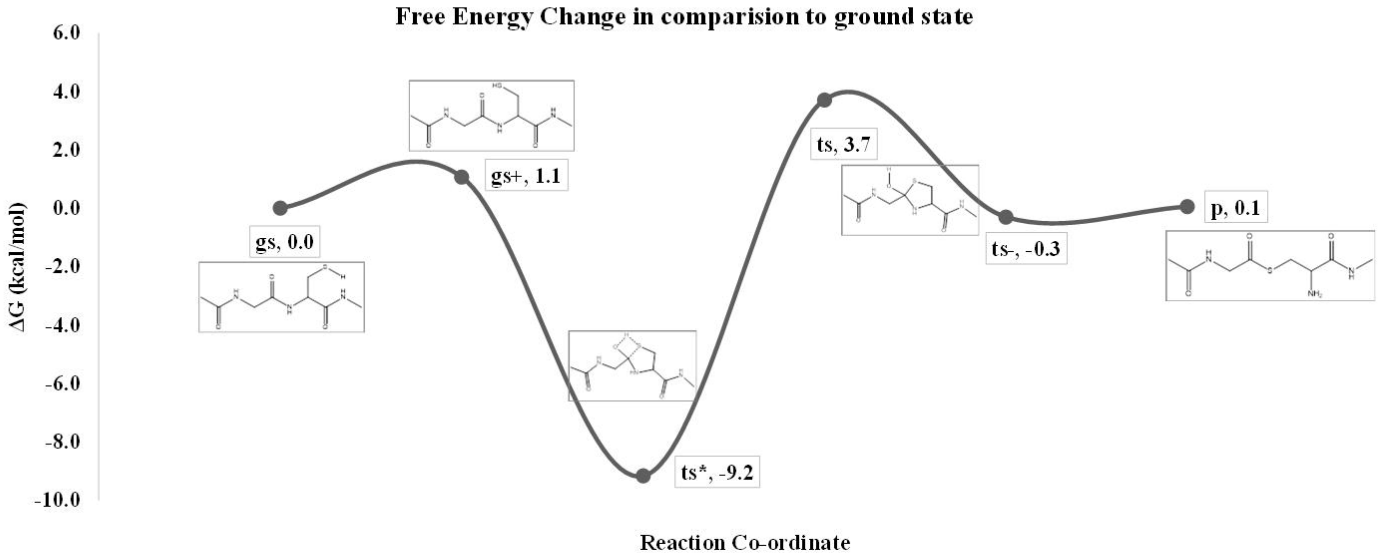
Free Energy Change in comparision to ground state
6.0
4.0
2.0
0.0
-2.0
-4.0
-6.0
-8.0
-10.0
ΔG (kcal/mol)
gs, 0.0
gs+, 1.1
ts*, -9.2
ts, 3.7
ts-, -0.3
p, 0.1
Reaction Co-ordinate

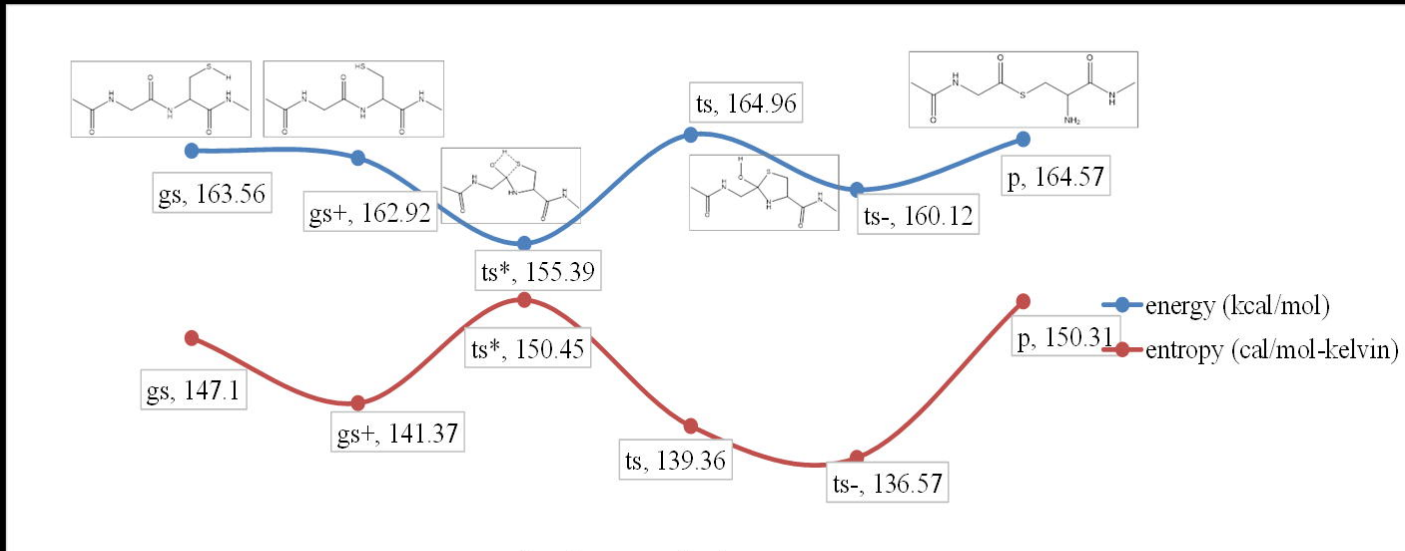
gs, 163.56
gs+, 162.92
ts*, 155.39
ts, 164.96
ts-, 160.12
p, 164.57
gs, 147.1
gs+, 141.37
ts*, 150.45
ts, 139.36
ts-, 136.57
p, 150.31
energy (kcal/mol)
entropy (cal/mol-kelvin)
Reaction co-ordinate